Numerical evaluation of the natural gamma radiation field at aerial survey heights

Løvborg, L.; Kirkegaard, P.

Publication date:
1975

Document Version
Publisher's PDF, also known as Version of record

Risø Report No. 317

Risø Report No. 317

Danish Atomic Energy Commission

Research Establishment Risø

Numerical Evaluation of the Natural Gamma Radiation Field at Aerial Survey Heights

by Leif Løvborg and Peter Kirkegaard

February 1975

Sales distributors: Jul. Gjellerup, 87, Sølvgade, DK-1307 Copenhagen K, Denmark

Available on exchange from: Library, Danish Atomic Energy Commission, Risø, DK-4000 Roskilde, Denmark

INIS Descriptors:

AERIAL MONITORING
ANGULAR DISTRIBUTION
COUNTING RATES
DOSE RATES
ENERGY SPECTRA
GAMMA RADIATION
GAMMA TRANSPORT THEORY
NATURAL RADIOACTIVITY
NUMERICAL SOLUTION
POTASSIUM
P1-APPROXIMATION
RADIATION FLUX
THORIUM
URANIUM

UDC 539.122.083:550.8:553.495:681.3

February 1975 Risø Report No. 317

Numerical Evaluation of the Natural Gamma Radiation Field at Aerial Survey Heights

by

Leif Løvborg

Electronics Department

and

Peter Kirkegaard

Computer Installation

Danish Atomic Energy Commission
Research Establishment Risø

Abstract

In computational studies of the count rates to be expected in airborne, radiometric surveys of geological formations, knowledge is required of the aerial gamma radiation field produced by the radioactive minerals in the ground. The data presented in this work permits calculation of the energy and angular distribution of the gamma-ray flux at distances of between 0 and 200 m from a plane, homogeneous ground with known abundances of thorium, uranium, and potassium. A tabulation permitting calculation of the gamma dose rate in the air is also given. The data are applicable to any normal ground material (rock or soil) in which uranium and thorium are in secular equilibrium with their respective daughters. Besides, the air density may have an arbitrary variation with the distance to the ground.

In calculating the flux of gamma rays that strike an airborne NaI(Tl) detector it is suggested to represent the bottom of the aircraft by an equivalent layer of air. For use in the numerical evaluation of aerial total count rates the angular gamma-ray flux at the point of detection is approximated in accordance with the double-P_1 polynomial expansion method. A detailed tabulation of flux expansion coefficients, calculated for 0.05-MeV wide energy intervals, is presented. To evaluate the differential count rates of high-energy Th-U-K gamma rays, it is convenient to make use of the well-known formulas for a flux of unscattered gamma rays. With this application in view data for insertion in these formulas are also given.

ISBN 82 550 0338 9

CONTENTS

		Page
1.	Introduction	5
2.	Model Assumptions and Sources of Basic Data	7
	2.1. The Terrain Considered	7
	2.2. Natural Gamma Ray Emitters	7
	2.3. Gamma Ray Interaction Cross Sections	9
3.	The Flux Concept and its Use in the Calculation of Aerial Detection Rates	11
	3.1. Angular Flux and Angular Counting Cross Section	11
	3.2. Scalar Flux and Average Counting Cross Section	13
4.	General Evaluation of the Aerial Gamma Radiation Field	14
	4.1. Double-P_1 Calculation of the Angular and the Scalar Flux	14
	4.2. Absorbed Dose Rate in the Air	15
	4.3. Numerical Example	16
	4.4. Extended Applications of the Flux and Dose Rate Data	20
5.	Evaluation of a Flux of Unscattered Gamma Rays	22
	5.1. Formulas and Data	22
	5.2. Numerical Example	24
6.	Method Suggested for the Calculation of Aerial Count Rates	25
7.	Discussion	28
References		29
Appendix I:	The Plane Gamma-Ray Transport Equation for Pure Compton Scatterers	31
Appendix II:	The Expansion Coefficients in the Double-P_1 Representation of the Angular Channel Flux	33
Tables		36

1. INTRODUCTION

Aerial prospecting for radioactive minerals is based on the use of large scintillation crystals (NaI(Tl) crystals) which are carried by aircraft at low altitudes to detect the gamma radiation emitted from the ground. The total crystal volume required for an airborne radiometric survey is dictated by counting statistics needs. Generally, the higher and faster it is necessary to fly, the larger the crystal volume must be. Besides a spectrometric data acquisition system requires more crystal volume than a system that only registers the gross count rate of gamma rays. Often the detector is composed of several crystal-photomultiplier assemblies operated in parallel. In the design of such a detector the question arises of how to choose the dimensions (diameter and thickness) of the individual scintillation crystals. Clearly one wishes to obtain the greatest possible aerial count rates per cubic centimetre of NaI(Tl) to be invested. For example, if a total of about 7000 cm^3 of NaI(Tl) is considered necessary for a particular survey, the detector could be designed on the basis of either four 6" x 4" crystals or three 8" x 3" crystals. In both cases the detector would contain 7413 cm^3 of NaI(Tl), but which of the two configurations would produce the highest count rates?

A problem similar to that presented above was experienced by the present authors several years ago when the Risø Electronics Department became involved in airborne uranium prospecting in Greenland. We therefore began computational studies of the response of NaI(Tl) detectors to natural, environmental gamma radiation. In these studies knowledge is required of the energy and angular distribution of the gamma rays striking the scintillation crystals. The part of our computational model describing the aerial radiation field produced by the radioactive minerals in the ground is now complete. Generally speaking, we have studied a plane, two-media gamma-ray transport problem, compiled basic data for use in the numerical solution of the transport equation, and prepared tables for straightforward, approximative determination of the angular gamma-ray flux in the air above ground material with known abundances of thorium, uranium, and potassium.

Gamma rays penetrating rocks and air are multiple-scattered, for which reason gamma-ray transport calculations are very complex even in plane, semi-infinite geometry. In the computational method used by us the flux of scattered gamma rays is divided into one component directed away from the ground and another component directed against the ground (the "skyshine" flux). Each of these components is represented by the zero'th

and the first order terms of an expansion of the angular gamma-ray flux in half-range Legendre polynomials. We have explained this so-called double-P_1 approximation in reference 1, in which we also describe the implementation of the flux calculation method in the form of a versatile data processing system, consisting of programs and data files. In reference 2 it was inferred, from spectrometric measurements in water on large, radioactive concrete slabs, that the data processing system is free from errors to within the limitations set by the quality of the basic data used and the accuracy of the double-P_1 approximation.

In this work we introduce the application of the double-P_1 approximation to the determination of the combined flux of scattered and unscattered gamma rays[x]. The resulting double-P_1 equations are presented in Chapter 4. Together with the flux expansion coefficients given in table 6 these equations are considered suitable for calculation of total gamma-ray count rates. In order to do so, the angular flux is multiplied by the angular counting cross section for the scintillation crystals, see reference 2, after which the product is integrated over all angles of incidence and over all energies above the counting threshold. As it may be of interest to compare the gross aerial count rate with the gamma dose rate, at the survey altitude or at ground level, we have included the dose rate values given in table 7.

Gamma-spectrometric, aerial surveys are normally based on a recording of the signals from differential counting channels centered at the energies 2.615, 1.765, and 1.461 MeV, characteristic respectively of thorium, uranium, and potassium. It is convenient to study these signals numerically from a calculation of the rate at which unscattered source gamma rays interact with the scintillation crystals in the airplane. With this application in view we present, in Chapter 5, data on the angular distribution of the significant unscattered flux components at the point of detection.

The information given in this report depends on several model assumptions and sources of basic data. In Chapter 2 we discuss the assumptions and make references to the data sources. The concepts of angular and scalar gamma-ray flux and the use of these field quantities in the evaluation of aerial detection rates are explained in Chapter 3. In Chapter 6 we outline our intended application of the data given in Chapters 4 and 5.

---

x) Calculation of the expansion coefficients is discussed in Appendix II.

2. MODEL ASSUMPTIONS AND SOURCES OF BASIC DATA

2.1. The Terrain Considered

The terrain to be surveyed radiometrically is supposed to have the following characteristics:

1. The ground material is homogeneous and infinite in extension.
2. The radioactive minerals are evenly dispersed in the ground.
3. The ground-air interface is plane.

Moreover, we neglect variations in the air density with distance to the ground (see, however, section 4.4).

In estimating the validity of these model assumptions we point out that most gamma rays emitted from the ground come from a shallow surface layer. Even a one metre thick formation can be regarded as infinite in the vertical direction. For the same reason a possible gradient in the depth distribution of the radioactive minerals just below ground level must be expected to influence the aerial gamma radiation field quite significantly, cf. the investigation by Beck and de Planque[3]. Whether the ground-air interface can be regarded as plane or not depends on the survey altitude. In the first place it must be demanded that the terrain be viewed at a solid angle that nearly equals 2π. Besides, the distance to the ground must be much greater than the magnitude of the natural terrain undulations.

Two common ground materials frequently encountered in aeroradiometric surveys are considered in this work: Soil and granite. The densitites and the chemical compositions ascribed to these materials are given in table 1. The soil data are identical to those chosen in reference 3, while the density and the composition of granite were taken from references 4 and 5 respectively.

2.2. Natural Gamma Ray Emitters

Table 1 shows that potassium oxide is the third most common constituent of a typical granite. This is because potassium forms common minerals like feldspar (orthoclase) and mica (muscovite and biotite). The spontaneous decay of the isotope ^{40}K (isotopic abundance 0.0119%) into stable ^{40}Ar by orbital-electron capture is followed by the emission of a gamma ray having the energy 1.461 MeV[6]. The values found in the literature for the specific gamma activity of potassium show a remarkable dispersion. Houtermans[7] reports 24 determinations made in the years 1947-1965. The values range

from 2.6 to 3.6 Y/(s · g). In this work we rely on the value of 3.30 Y/(s · g) presently recommended in the Nuclear Data Tables[8].

The radioactivity of thorium and uranium, whose normal abundances in granite are of the order of 10-20 ppm and 1-4 ppm respectively[9], is characterized by the decay chains formed by ^{232}Th, ^{238}U, and ^{235}U. Owing to its low isotopic abundance (0.71 % by weight), ^{235}U contributes little to the gamma-ray emission from a radioactive mineral[x]. The principal characteristics of the ^{232}Th and the ^{238}U decay chains are shown in tables 2 and 3. It is a basic assumption in this work that thorium and uranium are in secular equilibrium with their daughters anywhere in the ground. The gamma-ray emission spectra of ^{232}Th and ^{238}U with daughters were re-examined by Beck in 1972[11]. We have adopted his data together with the "best values" given by Hyde et al.[12] for the specific activities of the parent isotopes, i.e.

^{232}Th: 4100 dis/(s · g Th)

^{238}U: 12227 dis/(s · g U)[xx]

The most intensive gamma rays emitted by the daughters of thorium and uranium are listed in tables 4 and 5 in order of increasing energy. Whereas there are four significant gamma-ray emitters in the ^{232}Th decay chain, the great majority of uranium gamma rays comes from only two isotopes (^{214}Pb and ^{214}Bi). These are decay products of radon (^{222}Rn - ^{218}Po, see table 3). One of the most important sources of disequilibrium in the ^{238}U decay chain is the exhalation of radon from the ground into the air. This phenomenon is particularly pronounced for weathered, loosely-bound materials like soil. Assuming that one ^{222}Rn atom is typically exhaled from the ground per second, Jacobi and André[13] have derived the vertical distribution of radon and its daughters in the air under various meteorological conditions. The results were used by Beck[14] in a calculation of the gamma radiation field produced by airborne ^{214}Pb - ^{214}Bi. It was concluded that for normal atmospheric turbulence 2-5% of the gamma-ray flux above a thick layer of soil must be ascribed to radon emanating

---

x) The gamma-ray emission spectrum of ^{235}U + daughters adopted by us was derived from the most recent Atomic and Nuclear Data Tables[10]. From reference 2 it follows that more than 99% of the aerial gamma dose rate produced by uranium must be ascribed to daughters of ^{238}U.

xx) The specific activity of ^{235}U in natural uranium is 562 dis/(s · g U).

from the soil. In aeroradiometric prospecting radon in the air represents a source of gamma-ray background that has no interest in the present context.

2.3. Gamma Ray Interaction Cross-Sections

The energies of the gamma rays that strike an airborne NaI(Tl) crystal range from almost zero to 2.615 MeV. In recording the total gamma-ray count rate the counting threshold is normally set at a value of 0.1 MeV or greater, for which reason the flux of gamma rays with energies below 0.1 MeV is disregarded in this work. This means that we can confine the possible gamma-ray interactions in the ground and the air to the processes of incoherent (Compton) scattering, photoelectric effect, coherent scattering, and pair production. Our source of microscopic cross sections for these processes is the Livermore library DLC-7D[15] which is part of the U.S. evaluated nuclear data files. Of the elements determining the major composition of common rocks, iron is the one having the highest atomic number (Z = 26). The figures 1 and 2 show the relative contributions from the four principal interaction processes to the cross sections of the elements from hydrogen through iron for 0.1-MeV and 3-MeV gamma rays.

Following common practice in gamma-ray shielding calculations[16] we neglect the 0.511-MeV gamma radiation emitted when the positrons liberated in the pair-production process are annihilated in the ground and the air. Besides we consider coherent scattering a process that neither changes the direction nor the energy of the interacting gamma ray. The total macroscopic cross section $\mu(E)$ (the linear attenuation coefficient) for the material in question is consequently taken as the sum of the macroscopic cross sections for incoherent scattering, photoelectric effect, and pair production. The granite and the soil described in table 1 have average atomic numbers of 10.1 and 8.2 respectively, and the average atomic number for dry air is 7.2[a]. In the energy interval considered the photoelectric cross section is greatest for $E = 0.1$ MeV, while the pair-production cross section is greatest for $E = 3$ MeV. It follows from figures 1 and 2 that gamma rays predominantly interact with granite, soil and air by incoherent scattering. Therefore our gamma-ray transport model implies, typically, that the source gamma rays are deflected and degraded in energy by a series of scattering

---

[a] In this work air is assumed to consist of 79% nitrogen and 21% oxygen by weight.

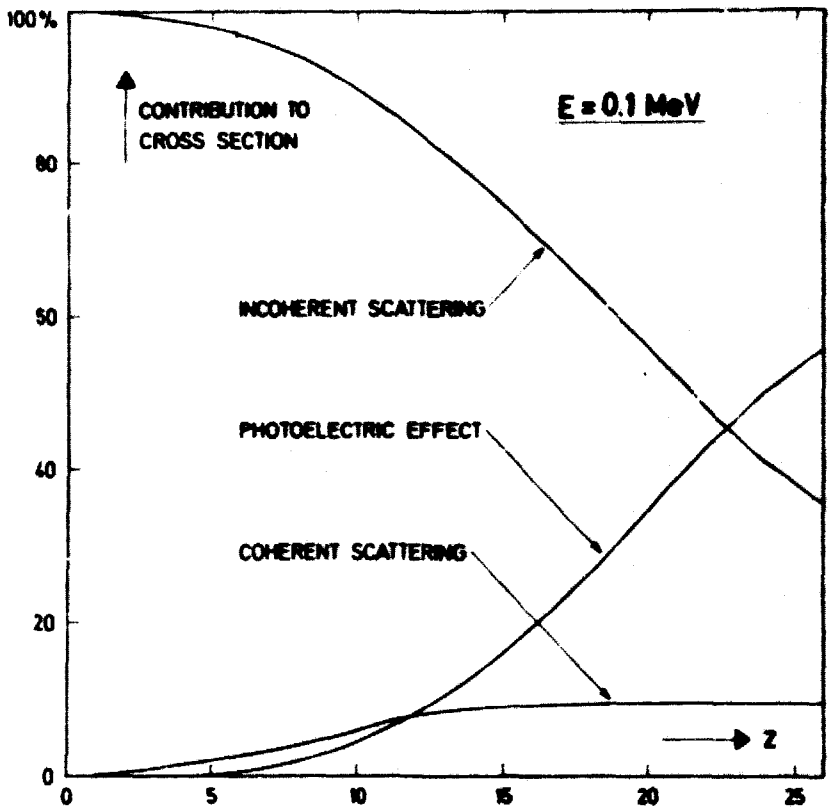

Fig. 1. Percentage contributions from incoherent scattering, photoelectric effect, and coherent scattering to the elemental interaction cross sections up to $Z = 26$ for gamma rays with the energy 0.1 MeV.

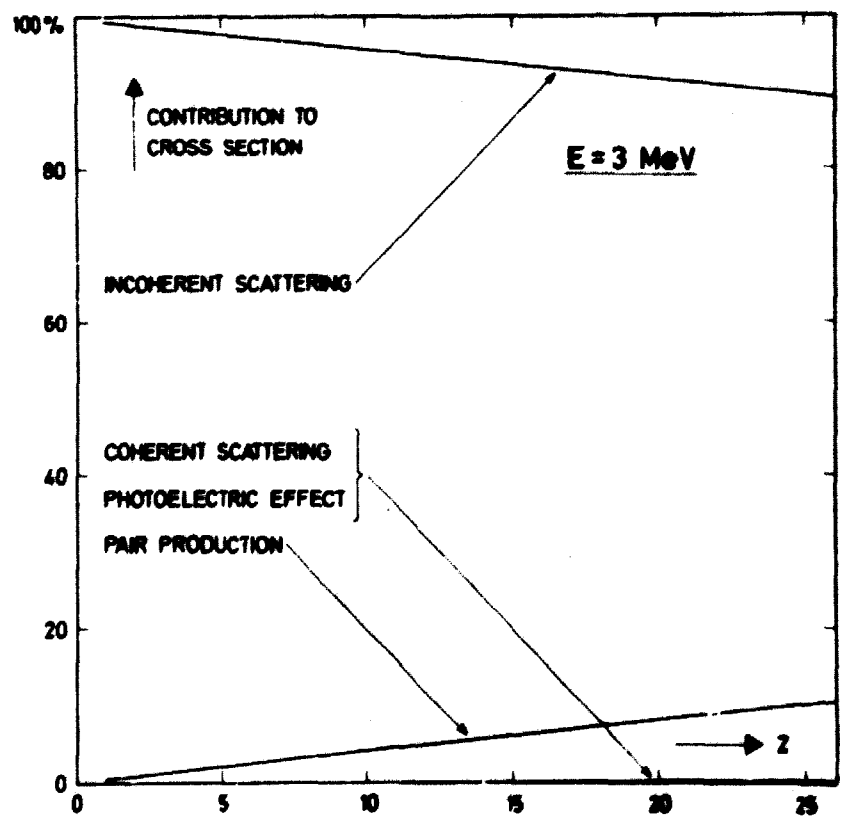

Fig. 2. Percentage contributions from incoherent scattering, pair production, coherent scattering, and photoelectric effect to the elemental interaction cross sections up to $Z = 26$ for gamma rays with the energy

events that terminates when the energy drops below 0.1 MeV. For each scattering event the relation between deflection angle and energy loss is described by Compton's well-known formula. The angular variation of the scattering cross section is given by the Klein-Nishina formula, see for example reference 16 or 1.

3. THE FLUX CONCEPT AND ITS USE IN THE CALCULATION OF AERIAL DETECTION RATES

3.1. Angular Flux and Angular Counting Cross Section

Consider a cylindrical NaI(Tl) crystal whose axis is oriented perpendicularly to the ground on board an aircraft flying at constant altitude z, see figure 3. It follows from the assumptions made in Chapter 2 that the gamma radiation field is constant along the flight line and axisymmetrical with respect to any vertical line. The latter implies that the angular properties of the field are fully described in terms of the polar angle θ between the vertical and the unit vector $\underline{\Omega}$.

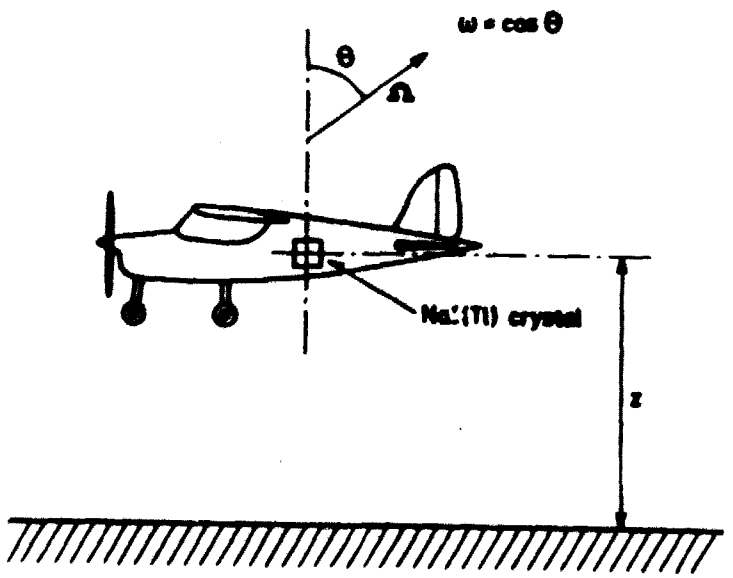

Fig. 3. Definition of the parameters z and ω used in the calculation of aerial detection rates.

Neglecting the gamma-ray attenuation in the aircraft structure, the differential rate of detection for the scintillation crystal can be written as

$$P(z, E) = \int_{4\pi} F(z, E, \omega)\,\sigma(E, \omega)\,d\underline{\Omega}\,, \tag{1}$$

where

$$\left.\begin{aligned} \omega &= \cos\theta \\ d\underline{\Omega} &= 2\pi d\omega = 2\pi \sin\theta\, d\theta \end{aligned}\right\}. \tag{2}$$

The function $F(z, E, \omega)$ describes the energy and angular distribution of gamma rays at the altitude z and will here for brevity be called the angular flux. $F(z, E, \omega)$ gives the number of gamma rays with energy E, travelling across a unit area perpendicular to $\underline{\Omega}$, per unit time, unit energy interval, and unit solid-angle element. The other function, $\sigma(E, \omega)$, entering the equation (1), is the angular interaction cross section (counting cross section) of the scintillation crystal for a broad parallel beam of gamma rays with energy E and direction $\underline{\Omega}$, see references 2 and 17, 18.

The angular flux is of fundamental importance for a detailed description of the radiation field. In order to calculate $F(z, E, \omega)$ above ground material with known abundances of thorium, uranium, and potassium, a time-independent gamma-ray transport equation (Boltzmann equation)[x] must be solved. If we characterize the emission lines from the radioelements in the ground by a sequence number (i), we can express $F(z, E, \omega)$ as the sum

$$F(z, E, \omega) = \sum_i F_i(z, E, \omega)\,, \tag{3}$$

where $F_i(z, E, \omega)$ is the angular flux resulting from the i'th emission line. In the transport equation for $F_i(z, E, \omega)$ the gamma rays that arrive at the point of detection without having been scattered in the ground material or the air are considered separately, i.e. the solution of the equation is written in the form

$$F_i(z, E, \omega) = u_i(z, \omega)\,\delta(E - E_i) + \phi_i(z, E, \omega)\,, \tag{4}$$

where E_i denotes the energy of the i'th emission line, and where δ stands for Dirac's delta function. The two terms on the right-hand side of formula (4) are the contributions to $F_i(z, E, \omega)$ from unscattered and scattered gamma rays respectively. The energy distribution of $\phi_i(z, E, \omega)$ is characterized by

---

x) Cf. references 1 and 16 and Appendix I.

having discontinuities at the energies E_i and $E_{ci} = E_i/(1 + 2E_i/0.511)$ (the Compton-edge energy). In the energy intervals from 0 to E_{ci} and from E_{ci} to E_i $\phi_i(z, E, \omega)$ is a continuous function of E.

3.2. Scalar Flux and Average Counting Cross Section

It is interesting to compare the differential detection rate P(z, E) for the actual NaI(Tl) crystal with the differential detection rate $P_o(z, E)$ for a hypothetical, spherical gamma-ray detector. The latter is defined as a detector whose angular counting cross section $\sigma_o(E)$ is constant in all directions, the value of $\sigma_o(E)$ being given by

$$\sigma_o(E) = \frac{1}{4\pi} \int_{4\pi} \sigma(E, \omega)\, d\underline{\Omega} . \tag{5}$$

The quantity on the right-hand side of formula (5) is the average counting cross section for the actual crystal, i. e. the angular counting cross section averaged over all angles of incidence. From formula (1) it follows that $P_o(z, E)$ can be written as

$$P_o(z, E) = N(z, E)\, \sigma_o(E) , \tag{6}$$

where

$$N(z, E) = \int_{4\pi} F(z, E, \omega) d\underline{\Omega} . \tag{7}$$

The function N(z, E) is the differential, scalar gamma-ray flux, in this work simply called the scalar flux, at the distance z from the ground.

The scalar flux is a useful quantity as it describes the overall energy distribution of the aerial radiation field as a function of the survey height. In analogy to formula (4), the scalar flux $N_i(z, E)$ contributed by the i'th gamma-ray emission line from thorium, uranium, or potassium is given by an expression of the form

$$N_i(z, E) = U_i(z)\delta(E-E_i) + \phi_i(z, E) , \tag{8}$$

where the two terms on the right-hand side are the scalar flux contributed by unscattered and scattered gamma-rays respectively.

4. GENERAL EVALUATION OF THE AERIAL GAMMA RADIATION FIELD

4.1. Double-P_1 Calculation of the Angular and the Scalar Flux

In describing the energy dependence of the flux quantities $F(z, E, \omega)$ and $N(z, E)$ we divide the energy range from 0.1 to 3 MeV into consecutive intervals of the width $\Delta E = 0.05$ MeV. Given the survey altitude z and the abundances of thorium, uranium, and potassium in the ground, we shall present data permitting calculation of the functions

$$\varphi(z, E, \omega) = \int_{I(E)} F(z, E', \omega)\, dE' \tag{9}$$

and

$$\Phi(z, E) = \int_{I(E)} N(z, E')\, dE', \tag{10}$$

where the integration is extended over that of the consesecutive intervals I(E) which contains E. In accordance with the similarity between the flux energy spectra thus defined and the spectra recorded with a multichannel analyser we shall call $\varphi(z, E, \omega)$ the angular channel flux and $\Phi(z, E)$ the scalar channel flux. These field quantities vary stepwise with the energy E, and they are expressed in units of $\gamma/(cm^2 \cdot s \cdot sterad)$ and $\gamma/(cm^2 \cdot s)$ respectively.

In the double-P_1 representation, on which our flux calculation method relies, the angular channel flux is given by the equations

$$\left.\begin{aligned} \varphi(z, E, \omega) &= \varphi^+(z, E, \omega) + \varphi^-(z, E, \omega) \\ \varphi^+(z, E, \omega) &\approx \varphi_0^+(z, E) + 3\varphi_1^+(z, E)(2\omega - 1) \\ \varphi^-(z, E, \omega) &\approx \varphi_0^-(z, E) + 3\varphi_1^-(z, E)(2\omega + 1) \\ \omega &= \cos\theta \quad \text{(figure 3)}. \end{aligned}\right\} \tag{11}$$

The first equation expresses that the flux is taken as a sum of two components, $\varphi^+(z, E, \omega)$ and $\varphi^-(z, E, \omega)$. The former is defined to be equal to $\varphi(z, E, \omega)$ for $0 < \omega \leq 1$ $(0 \leq \theta < \frac{\pi}{2})$ and to be zero otherwise. Conversely $\varphi^-(z, E, \omega)$ equals $\varphi(z, E, \omega)$ for $-1 \leq \omega < 0$ $(\frac{\pi}{2} < \theta \leq \pi)$ and zero otherwise. This implies that $\varphi_0^+(z, E, \omega)$ is the flux contributed by gamma rays

travelling away from the ground, while $\varphi^-(z, E, \omega)$ is to be interpreted as a flux of gamma rays that have been backscattered against the ground at aerial heights greater than z. The next two equations show that the two flux components are approximated by linear expressions in $2\omega - 1$ and $2\omega + 1$ respectively. Such an approximation corresponds to an expansion of $\varphi(z, E, \omega)$ in half-range, spherical harmonics[1] where only the zero'th and the first order expansion terms are retained. The polynomials in which $\varphi(z, E, \omega)$ is expanded are orthogonal, from which it follows that the scalar channel flux only depends on the zero'th order terms in the expansion:

$$\Phi(z, E) = 2\pi \left\{ \varphi_0^+(z, E) + \varphi_0^-(z, E) \right\}. \qquad (12)$$

Table 6 gives the flux expansion coefficients $\varphi_0^+(z, E)$, $\varphi_1^+(z, E)$, $\varphi_0^-(z, E)$, and $\varphi_1^-(z, E)$ at aerial survey heights of z = 25, 50, 75, ..., 200 m. Since it is of general interest to compare the radiation field at the actual survey altitude with the radiation field near the ground level, table 6 also includes the expansion coefficients for z = 0 and z = 1 m. The table was prepared at the Risø Computer Installation using the multi-file tape GAMMA-BANK and the program GAMPI described in reference 1. In constructing table 6 it was decided to represent the ground material by granite (table 1) and to ascribe a density of 0.001293 g/cm^3 to the air, corresponding to an atmospheric pressure of 1 atm and a temperature of 0°C[x]. To permit calculation of the gamma-ray flux produced by arbitrary contents of thorium, uranium, and potassium in the ground, table 6 includes three sets of flux expansion coefficients, giving, respectively, the contribution to the flux from 1 ppm Th, 1 ppm U, and 1% K. An example of the use of table 6 is given in section 4.3. The applicability of the flux expansion coefficients in cases where the ground does not consist of granite, and where the density of the air is different from 0.001293 g/cm^3, is discussed in section 4.4.

4.2. Absorbed Dose Rate in the Air

One of the basic problems in aeroradiometric prospecting is to correlate the total count rate of gamma rays with the overall abundance of the radioactive minerals in the ground. The results reported in reference 2 indicate that for a certain setting of the counting threshold the total gamma-ray count rate will be almost proportional to the aerial gamma dose rate at the

[x] Temperatures close to freezing point are characteristic of the conditions for airborne uranium prospecting in Greenland.

survey altitude, *independent of the ratio* Th:U:K for the ground material. If this assumption is valid, aerial gross count rates can be converted into dose rate units. Moreover, if the decrease in the dose rate with the distance to the ground is known, it should be possible to deduce the dose rate at ground level, the quantity that appears to be the most suitable measure of the radioactivity of the ground.

The absorbed gamma dose-rate D(z) at the survey altitude z is given by

$$D(z) = \int_0^{E_{max}} N(z, E)\, \mu_{ea}(E)\, E\, dE \qquad (13)$$

with $E_{max} = 2.615$ MeV. In this formula N(z, E) is the scalar gamma-ray flux, while $\mu_{ea}(E)$ (cm^2/g) is the energy absorption coefficient[16] for air. Our program GFX permits calculation of D(z) expressed in units of $MeV \cdot g^{-1} \cdot s^{-1}$. Using the same reference conditions as in the preceding section, table 7 was constructed, in which the values of D(z) are given in units of μrad/h (1 rad = 6.242×10^7 MeV/g). As is well known, gamma doses (in rads) received by people are numerically equal to the radiation exposure measured in Röntgen units (R). The absorbed dose in standard air (0°C, 1 atm) is related to the radiation exposure by the conversion equation

$$1\ R = 0.869\ rad, \qquad (14)$$

which relies on the assumption that 33.7 eV is required to create one ion pair[19]. Though radiometric instruments for geological field work are often calibrated in exposure rate units, we find it more natural to state the results of total gamma-ray measurements in dose rate units.

4.3. Numerical Example

To evaluate an aerial gamma radiation field, the respective flux and dose rate data in tables 6 and 7 are to be combined in accordance with the actual abundances of thorium, uranium, and potassium in the ground. The granite for which the tables were derived contains 4.11% K_2O (table 1), corresponding to 3.412% K. In the following we assume that the abundances of thorium and uranium in the granite are 12 ppm and 3 ppm respectively. The energy distributions of the resulting flux expansion coefficients $\varphi_0^+(z,E)$ and $\varphi_0^-(z, E)$ for z = 1 m and z = 100 m are shown in figures 4 and 5. It will be recalled that $\varphi_0^+(z, E)$ gives the flux of gamma rays travelling away

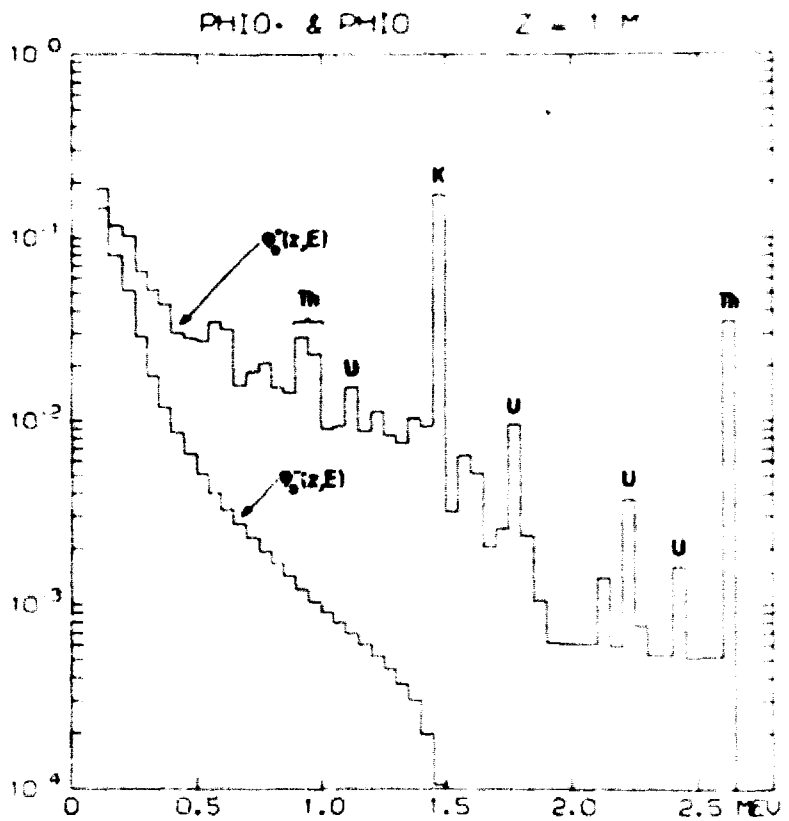

Fig. 4. The energy distribution of the flux expansion coefficients $\varphi_0^+(z, E)$ and $\varphi_0^-(z, E)$ at the altitude z = 1 m above granite containing 12 ppm Th, 3 ppm U, and 3.41 2% K.

from the ground, while $\varphi_0^-(z, E)$ represents the "skyshine" contribution to the flux. Since $\varphi_0^+(z, E)$ includes the expansion coefficients for the flux of unscattered gamma rays, the graphs of $\varphi_0^+(z, E)$ are characterized by peaks. The most prominent peaks in the two figures are labelled according to the radioelements by which they are produced.

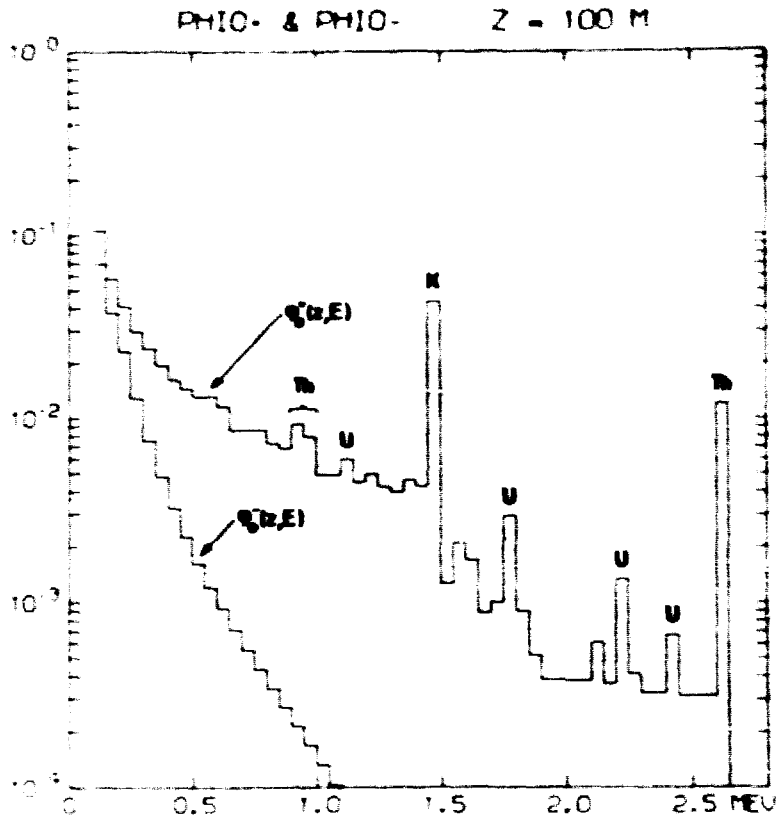

Fig. 5. The energy distribution of the flux expansion coefficients $\varphi_0^+(z, E)$ and $\varphi_0^-(z, E)$ at the altitude z = 100 m above granite containing 12 ppm Th, 3 ppm U, and 3.412% K.

Fig. 6 shows the variation of the angular channel flux $\varphi(z, E, \omega)$ with the polar angle ϑ for E = 0.125 MeV at the altitudes z = 1 m and z = 100 m. Since none of the emission lines of the natural radioelements have energies in the interval from 0.10 to 0.15 MeV, the figure exemplifies the angular properties of a flux of scattered low-energy gamma rays. The small jumps seen in the graph of $\varphi(z, E, \omega)$ for z = 1 m in the transition from positive to negative values of $\omega = \cos\vartheta$ arise fromthe truncation error in the double-P_1 approximation. It is seen that close to the ground (z = 1 m) the gamma-ray flux per steradian varies less than a factor of two as ϑ is increased from 0 to π. At both altitudes considered the contribution from "skyshine" ($\frac{\pi}{2} < \vartheta \leq \pi$) to the scalar channel flux amounts to about 40%.

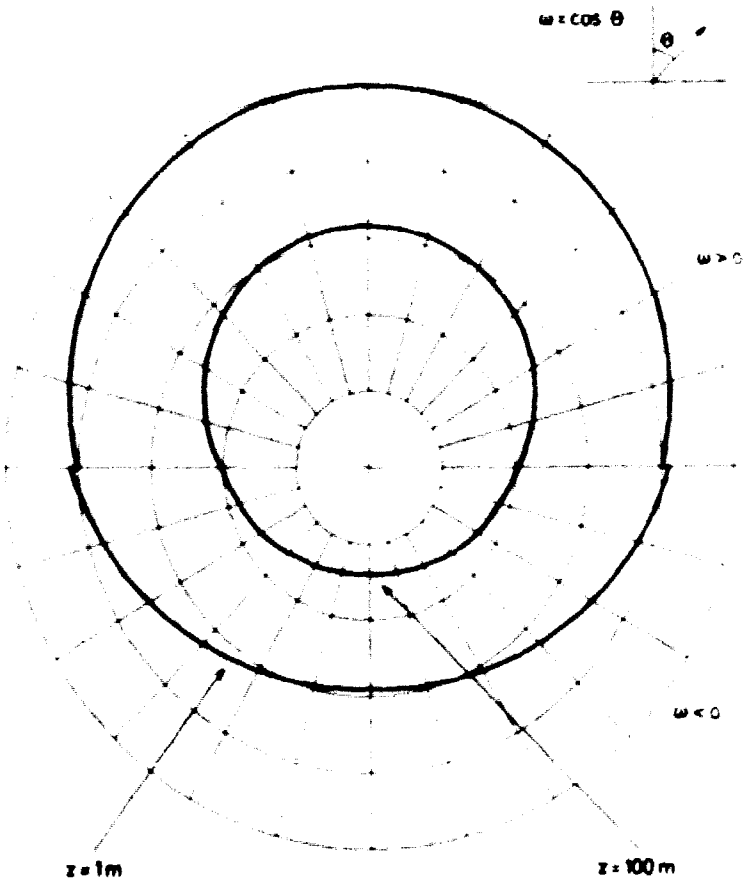

Fig. 6. The variation of the angular channel flux ($\gamma/cm^2 \cdot s \cdot$ sterad)) with the polar angle θ in the energy interval from 0.10 to 0.15 MeV at the altitudes z = 1 m and z = 100 m.

In fig. 7 we illustrate the relative diminuation in the total gamma-ray flux $\Phi_{tot}(z)$ and the dose rate D(z) resulting from an increase in z from 0 to 200 m. Since gamma rays with energies of less than 0.1 MeV are disregarded in this work, the total gamma-ray flux is given by

$$\Phi_{tot}(z) = \int_{E_{min}}^{E_{max}} N(z, E)dE = 2\pi \left\{ \Sigma \varphi_o^+(z, E) + \Sigma \varphi_o^-(z, E) \right\} \quad (15)$$

with E_{min} = 0.1 MeV and E_{max} = 2.615 MeV. Values of $\Sigma \varphi_o^+(z, E)$ and $\Sigma \varphi_o^-(z, E)$ are derivable from the rows labelled "sum" in table 6. The figure shows that the total flux decreases less rapidly with altitude than the dose rate. The reason is that the multiple scattering events cause the spectrum of gamma rays to be shifted towards lower energies as the aerial altitude increases.

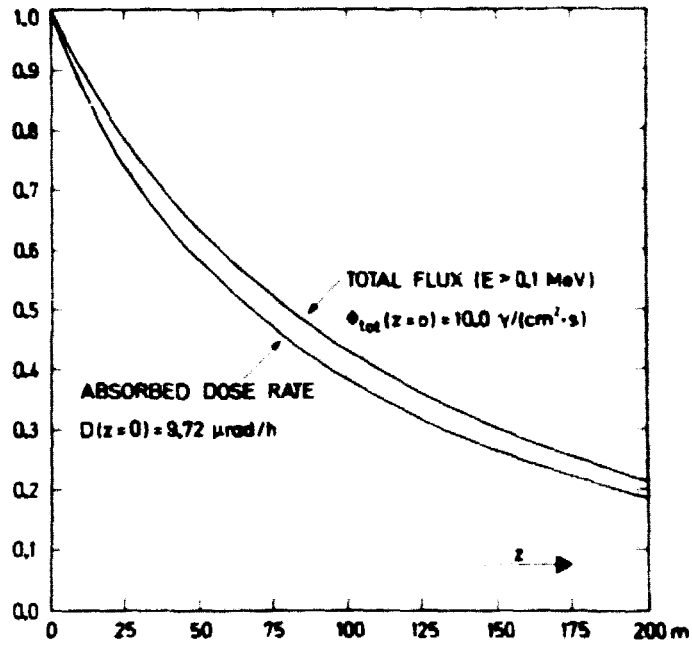

Fig. 7. The relative diminuation in the total gamma-ray flux and the gamma dose rate with the distance z to ground material (granite) containing thorium, uranium, and potassium in the proportions 12:3:34120.

4.4. Extended Applications of the Flux and Dose Rate Data

After having presented data on the flux and the dose rate in standard air above granite of the composition given in table 1, we shall now show that tables 6 and 7 can be used for approximate calculation of the gamma radiation field produced by all normal ground materials in air of arbitrary density. Moreover, it will appear that the radiation field can be evaluated even if the air density varies with altitude. Since the main purpose of this work is to establish a basis for the calculation of aerial count rates, we shall also mention how the structural materials surrounding an airborne NaI(Tl) detector can be taken into consideration. The following discussion is based on the fact that soil and all common rocks, the atmosphere, and most of the materials used in an aircraft and a detector housing consist of elements with low atomic numbers ($Z \leq 26$). In section 2.3 it was pointed out that gamma rays with energies of between 0.1 and 3 MeV interact with low-Z elements almost exclusively by incoherent scattering. It appears from Appendix I that the electron densities for the materials involved are essential in describing the transport of gamma rays through pure Compton scatterers. The electron density n_e for a homogeneous material is given by

$$n_e = \rho N_o \sum_i w_i \frac{Z_i}{A_i}, \qquad (16)$$

where

ρ = bulk density of the material

N_o = Avogadro's number (6.025×10^{23})

(w_i, Z_i, A_i) = (abundance by weight, atomic number, atomic weight) for the i'th element in the compositional code for the material.

It follows from the formulas (A5) and (A6) in Appendix I that the radiation field above a uniform mixture of Compton scatterers with electron density n_e and gamma-ray emitters with source density q is proportional to the ratio q/n_e. This implies that the aerial radiation field produced by unit weight concentrations of thorium, uranium, or potassium in the ground is inversely proportional to the quantity

$$\left\langle \frac{Z}{A} \right\rangle = \sum_i w_i \frac{Z_i}{A_i} \qquad (17)$$

for the ground material. The granite for which tables 6 and 7 were derived has $\left\langle \frac{Z}{A} \right\rangle = 0.4965$. Therefore, to determine the flux and the dose rate above a ground having another value of $\left\langle \frac{Z}{A} \right\rangle$, the figures in the two tables should in principle be multiplied by a factor of $0.4965/\left\langle \frac{Z}{A} \right\rangle$. Generally the correction is quite small and can often be omitted. This is because the quantity $\frac{Z_i}{A_i}$ varies by as little as from 0.4551 (manganese) to 0.5000 (oxygen) for the elements, with the exception of hydrogen, which enter the common rock-forming minerals. For example, the value of $\left\langle \frac{Z}{A} \right\rangle$ for the soil described in table 1 is 0.5026, so the field quantities per 1 ppm Th, 1 ppm U, and 1% K are only 1.2% smaller for soil than for granite. Since hydrogen has $\frac{Z_i}{A_i} = 0.9921$ it may be necessary to include the correction in calculating the radiation field above material that is soaked with water.

The formulas (A4) and (A5) (Appendix I) show that the vertical distribution of the gamma-ray flux in an assembly of Compton scatterers, whose electron density $n_e(z)$ varies with the distance z to a plane, infinite source medium, is a function of the total number of electrons per cm^2 in a vertical column of the height z. If we let the Compton scatterers represent the atmosphere, it follows that tables 6 and 7 permit calculation of the radi-

ation field in air whose density varies according to a function $\rho(z)$. Thus, if z_1 denotes one of the altitudes for which the flux expansion coefficients and the dose rate are tabulated, these field quantities are the same at the altitude z_2 in the air characterized by the function $\rho(z)$, where z_2 is derivable from the equation

$$0.001293 \cdot z_1 = \int_0^{z_2} \rho(z')dz' . \qquad (18)$$

In the normal case in which the air density can be regarded as constant, $\rho(z) = \rho$, at altitudes of between 0 and ~200 m, z_2 is simply given by

$$z_2 = z_1 \cdot 0.001293/\rho . \qquad (19)$$

If the air temperature t (^{o}C) and the atmospheric pressure p (atm) are specified, ρ is calculated by means of the well-known expression

$$\rho = 0.001293 \frac{p}{1 + t/273} . \qquad (20)$$

In order to evaluate the flux of gamma rays that strikes an airborne NaI(Tl) detector one has to calculate the total number of electrons per cm^2 in all material present between the detector and the ground. In such a calculation it is convenient to express the thickness of the detector housing and the bottom of the aircraft as an equivalent layer of air which has to be added to the survey altitude. For example, a 1 cm thick layer of an aluminium alloy having a density of 2 g/cm^3 is equivalent to a 15 m high column of standard air. We point out that only the upwards-directed gamma-ray flux, expressed by the expansion coefficients $\varphi_0^+(z, E)$ and $\varphi_1^+(z, E)$ in table 6, is influenced by the structural materials surrounding the detector. The "skyshine" flux is unchanged, because its energy and angular distribution are independent of the position of the scattering electrons above the point of detection.

5. EVALUATION OF A FLUX OF UNSCATTERED GAMMA RAYS

5.1. Formulas and Data

In this chapter we shall present data for insertion in the well-known formulas for a flux of unscattered gamma rays. We have previously (Chapter 3) introduced the quantities $u_i(z,\omega)$ and $U_i(z)$, describing the

the angular and the scalar flux produced by source gamma rays of the energy E_i. The formulas (4) and (8) show that $u_i(z,\omega)$ and $U_i(z)$ are expressed in units of $\gamma/(cm^2 \cdot s \cdot sterad)$ and $\gamma/(cm^2 \cdot s)$ respectively. The expressions for $u_i(z,\omega)$ and $U_i(z)$ can be written as (cf. reference 2)

$$\left.\begin{aligned} u_i(z,\omega) &= \frac{Q_i}{4\pi\,\mu_m^G(E_i)}\,\exp(-x/\omega) \\ U_i(z) &= \frac{Q_i}{2\,\mu_m^G(E_i)}\,E_2(x)\,, \end{aligned}\right\} \qquad (21)$$

where

ω = $\cos\theta$ ≥ 0 (fig. 3)

x = $\mu_m^A(E_i)\,\rho\,z$

ρ = density of the air

$\mu_m^A(E_i)$ = total cross section without coherent scattering for air, in cm^2/g

$\mu_m^G(E_i)$ = ditto for the ground material

Q_i = emission rate of gamma rays with energy E_i per gram of the ground material.

The cross sections $\mu_m^G(E_i)$ and $\mu_m^A(E_i)$ are often referred to as the mass attenuation coefficients for the ground and the air. The function $E_2(x)$ is a special case of the exponential integral of the order n:

$$E_n(x) = x^{n-1}\int_x^\infty \exp(-t)/t^n\,dt = \int_0^1 \omega^{n-2}\exp(-x/\omega)d\omega\,. \qquad (22)$$

$E_2(x)$ has been tabulated, for example, by Trubey[20]. In fig. 8 we show the graph of $E_2(x)$ for $0 \le x \le 3.5$.

Table 8 shows the values of Q_i, normalized to abundances of 1 ppm Th or 1 ppm U in the ground material, for the thorium-uranium gamma rays whose energies and intensities are listed in tables 4 and 5. The value of Q_i for potassium (1 % K) is also given. Besides, table 8 gives the mass attenuation coefficients of granite, soil (cf. table 1), and air for the gamma-ray energies in question. The mass attenuation coefficients were calculated by means of the data file GAMMABANK and the program GBCROS[1]. For material that can be regarded as a pure Compton scatterer, the mass

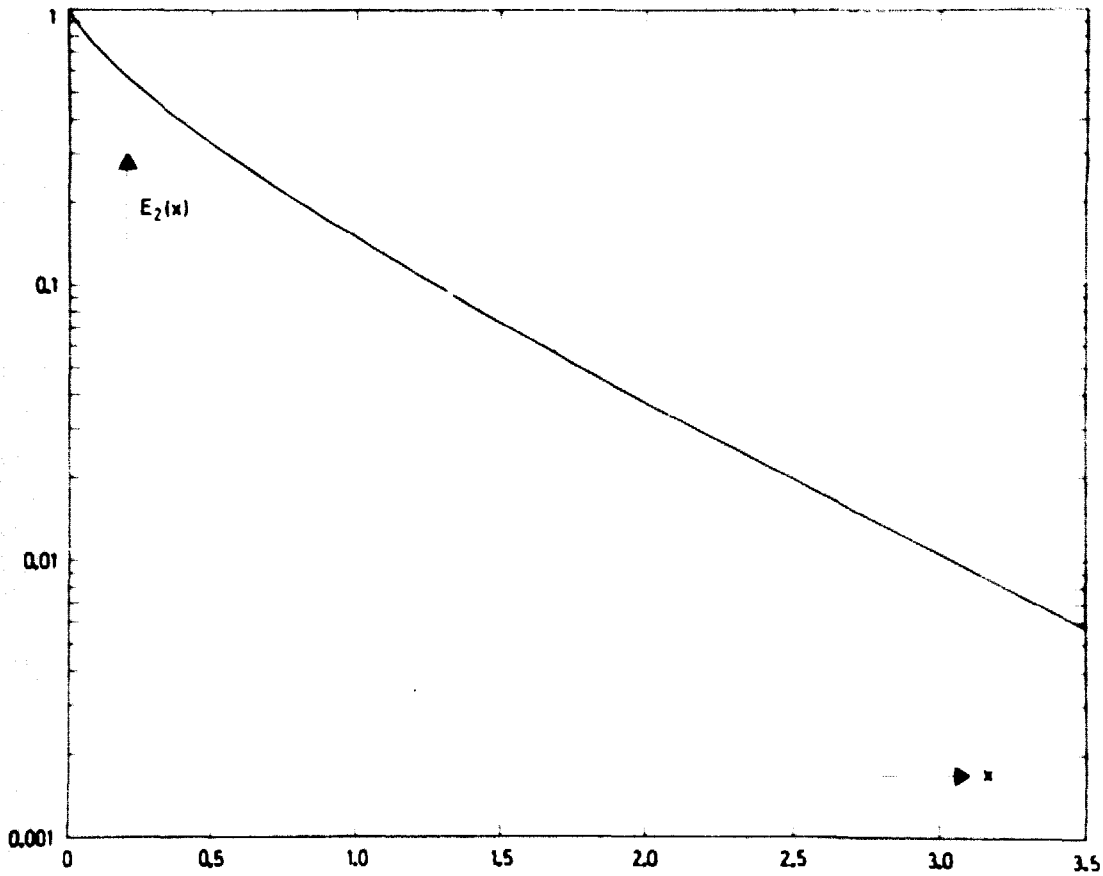

Fig. 8. Graph of the second-order exponential integral $E_2(x)$ entering formula (21).

attenuation coefficient is proportional to the quantity $\langle \frac{Z}{A} \rangle$ defined by formula (17). The ratios between the values of $\langle \frac{Z}{A} \rangle$ for granite, soil, and air equal 1:1.012:1.007, and since the ratios between the three sets of mass attenuation coefficients in table 6 are in fair agreement with this proportion, the table further illustrates the fact that incoherent scattering is the predominant gamma-ray interaction process in typical ground materials and air.

5.2. Numerical Example

Fig. 9 exemplifies the variation of the angular flux of unscattered 2.615-MeV gamma rays from thorium with the polar angle θ. The plot pertains to granite and standard air ($\rho = 0.001293$ g/cm^3). As one would expect, the flux distribution is upward peaked at aerial survey altitudes ($z = 100$ m) but nearly half-isotropic close to the ground ($z = 1$ m). It may be useful to introduce the fraction α of gamma rays whose directions are confined to the interval from $\theta = 0$ to $\theta = \theta_0$. Given α, the angle θ_0 =

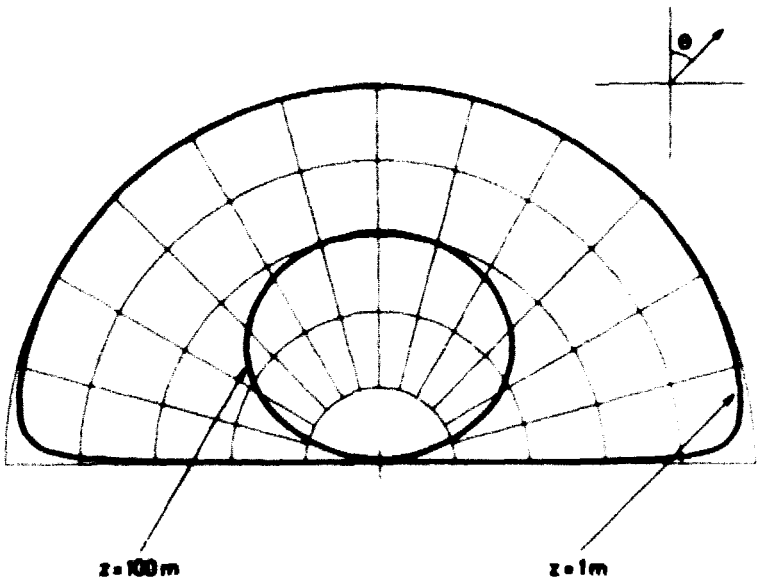

Fig. 9. The variation of the angular flux ($\gamma/cm^2 \cdot s \cdot sterad \cdot MeV$)) of unscattered 2.615 - MeV gamma rays at the altitudes z = 1 m and z = 100 m.

$\theta_o(z, E_i, a)$ is derivable from the equation

$$\frac{E_2(x/\cos\theta_o)}{E_2(x)} \cos\theta_o = 1 - a, \qquad (23)$$

where x is given by formula (21) ff. Since z and θ_o define a cone whose intersection with the air-ground interface is a circle with the radius $R = z \tan\theta_o$, the interface can be divided into concentric, circular areas, each contributing a specified fraction of the scalar flux at the survey altitude considered ("circles of investigation", cf. reference 21). In the present example we find for a = 0.5 that (θ_o, R) = (45°, 101 m) at z = 100 m and (θ_o, R) = (59°, 1.7 m) at z = 1 m.

6. METHOD SUGGESTED FOR THE CALCULATION OF AERIAL COUNT RATES

We have now concluded the main objective of this report, namely to introduce formulas and tables for numerical evaluation of the aerial gamma-ray flux from the radioactive minerals in rock or soil making up a plane, uniform terrain. Since the data have been compiled with a view to their application in the optimum design of airborne NaI(Tl) detectors, cf. chapter 1, we shall round off the report by briefly mentioning the

method we intend to use for the calculation of aerial count rates.

The first of the simplifying assumptions on which the method relies is that the pulse-height spectrum derived from a detector, which consists of two or more crystal-photomultiplier units, is the sum of the pulse-height spectra produced by the individual units. In other words, we neglect the screening and the scattering effects in an array or a block of airborne scintillation crystals. Let $f(z, V)$ be the count rate of pulses with amplitudes between V and V + dV obtained with a single NaI(Tl) crystal flown in an aircraft at the altitude z (fig. 3). The spectrum $f(z, V)$ can be written as

$$f(z, V) = 2\pi \int_0^{E_{max}} \int_{-1}^{1} F(z, E, \omega)\, \sigma(E, \omega)\, G(E, V, \omega)\, d\omega\, dE \qquad (24)$$

with $E_{max} = 2.615$ MeV. $F(z, E, \omega)$ denotes the angular gamma-ray flux at the point of detection. In section 4.2 we have explained how the gamma-ray attenuation in the aircraft structure and the detector housing can be taken into consideration in the calculation of $F(z, E, \omega)$. The angular counting cross section $\sigma(E, \omega)$ for the NaI(Tl) crystal has been defined in section 3.1. The third function, $G(E, V, \omega)$, appearing in the formula is the response function for the crystal-photomultiplier assembly. $G(E, V, \omega)$ is to be interpreted as a normalized pulse-height spectrum, generated by a parallel beam of gamma rays having the energy E and forming an angle of $\theta = \arccos\omega$ with the crystal axis. As is well known, monoenergetic gamma rays interacting with a NaI(Tl) crystal are either totally absorbed, in which case they give rise to a full-energy peak (and two annihilation escape peaks if the energy is greater than 1.022 MeV), or they are scattered out of the crystal whereby a Compton continuum is formed.

As the next simplifying assumption we disregard the angular dependence of the response function, i.e. we set

$$G(E, V, \omega) = G(E, V). \qquad (25)$$

It is common practice to write $G(E, V)$ as the convolution of an energy deposition spectrum $D(E, E')$ and a Gaussian resolution function $R(E', V)$, i.e.

$$G(E, V) = \int_0^E D(E, E')\, R(E', V)\, dE' . \qquad (26)$$

Thus, to calculate an aerial pulse-height spectrum knowledge is required of the following quantities describing the performance of the detector unit:

1. The angular counting cross section $\sigma(E,\omega)$
2. The components of the function D(E, E')
   (photofraction, escape-peak intensities,
   and parameters characterizing the Compton continuum
3. The parameters giving the width at half maximum
   (FWHM) of the function R(E', V).

Whereas the calculation of angular counting cross sections is a comparatively simple numerical problem, cf. reference 18, energy deposition spectra must be evaluated from extensive Monte Carlo calculations, or they must be determined experimentally. In reference 2 we have derived the response function for a 3" x 3" NaI(Tl) detector using information on D(E, E') available in the literature. As far as we know, detailed response-function data for large scintillation detectors have not been published so far, and therefore further approximations have to be introduced.

Even the most advanced aeroradiometric recording systems rarely sort the detector pulses into more than four counting channels. Of these one is used for measurement of the total gamma-ray count rate, while the three others form a gamma spectrometric data acquisition system, by means of which one endeavours to determine the abundances of thorium, uranium, and potassium in the terrain beneath the aircraft. Normally the spectrometer channels are about 0.2-MeV wide and centered at the energies 2.615, 1.765, and 1.461 MeV respectively, cf. section 2.2. In an attempt to determine the optimum crystal dimensions for a recording system to be flown at a given altitude, it is reasonable to confine the examination to the integral counting channel and the differential counting channel with centre energy 2.615 MeV. Recalling that P(z, E) denotes the rate of detection for the scintillation crystal (section 3.1), the following approximate formulas can be established for the total count rate $n_{tot}(z)$ and the differential count rate $n_{2.615}(z)$:

$$n_{tot}(z) = \int_{E_o}^{\infty} f(z, V)dV \approx \int_{E_o}^{E_{max}} P(z, E)dE$$

$$\approx 2\pi \sum_i \int_{-1}^{1} \varphi(z, E, \omega)\, \sigma(E, \omega)d\omega \qquad (27)$$

$$n_{2.615}(z) \approx 2\pi\, p_o(E_i) \int_o^1 u_i(z, \omega)\, \sigma(E_i, \omega)d\omega\,. \qquad (28)$$

In formula (27) E_o is the counting threshold expressed in MeV, while $\varphi(z, E, \omega)$ is the angular channel flux given by the double-P_1 equations (11). In the last expression in (27), the symbol $\sum_i$ is understood as a summation over the "energy channels" of width $\Delta E = 0.05$ MeV introduced in section 4.1, beginning with the channel to which E_o belongs. Formula (28) expresses that $n_{2.615}(z)$ is taken as the count rate in the total absorption peak produced by unscattered 2.615-MeV gamma rays from thorium (cf. formula (21) and table 8). Therefore both the counting cross section $\sigma(E_i, \omega)$ and the photofraction $p_o(E_i)$ must be known for $E_i = 2.615$ MeV.

7. DISCUSSION

It may be questioned whether the double-P_1 representation of the angular channel flux (formula (11)) is sufficiently accurate for determination of aerial total gamma-ray count rates (formula (27)). To comment on this problem we first observe that two types of error occur:

(i) No harmonics of order $l > 1$ are retained in the expansion of the flux.

(ii) The calculation of the zero'th and the first harmonics is not exact, cf. reference 1.

Errors of both types will affect the accuracy of response calculations for anisotropic detectors, whereas only type (ii) errors will do so in the case of an isotropic (spherical) detector[x]. Regarding the scattered flux,

[x] The accuracy of the dose rate values in table 7 also exclusively depends on type (ii) errors.

which varies rather slowly in the intervals $-1 \leq \mu < 0$ and $0 < \mu \leq 1$, we have strong evidence[1,2] that the type (ii) errors are small; for the unscattered flux they are zero. Again, errors of type (i) are expected to be small for the scattered flux, but unfortunately this is not true for the unscattered flux. In fact, we have to admit that the angular distributions of the unscattered flux (graphs like those in fig. 9) are rather poorly reproduced by retaining only the terms $l = 0$ and $l = 1$ in the double-P_l expansion (cf. Appendix II). We believe, nevertheless, that the error introduced by the strong anisotropy of the unscattered flux can be tolerated, because the numerical evaluation of formula (27) involves integration with respect to directions and summation over energy intervals, by which the error tends to be diluted.

REFERENCES

1) P. Kirkegaard and L. Løvborg, Computer Modelling of Terrestrial Gamma-Radiation Fields. Risø Report No. 303 (1974) 88 pp.

2) L. Løvborg and P. Kirkegaard, Response of 3" x 3" NaI(Tl) Detectors to Terrestrial Gamma Radiation. Nucl. Inst. Meth. 121 (1974) 239-251.

3) H. Beck and G. de Planque, The Radiation Field in Air due to Distributed Gamma-Ray Sources in the Ground. HASL-195 (1968) 53 pp.

4) R.A. Daly, G.E. Manger, and S.P. Clark, Jr., in: Handbook of Physical Constants. Revised edition. Edited by S.P. Clark, Jr. (Geological Society of America, New York, 1966) 19-26.

5) S.P. Clark, Jr., ibid 1-5.

6) J.D. King, N. Neff, and H.W. Taylor, The Energy of the ^{40}K Gamma Ray and its Use as a Calibration Standard. Nucl. Inst. Meth. 52 (1967) 349-350.

7) F.G. Houtermans, in: Potassium Argon Dating. Edited by O.A. Schaeffer and J. Zähringer (Springer Verlag, Berlin, 1966) 1-6.

8) M.J. Martin and P.H. Blichert-Toft, Radioactive Atoms. Nucl. Data Tables A8 (1970) 1-198.

9) J.J.W. Rogers and J.A.S. Adams, in: Handbook of Geochemistry. Edited by K.H. Wedepohl. Vol. II/2 (Springer Verlag, Berlin, 1970). Chapters 90 and 92.

10) W. W. Bowman and K. W. MacMurdo, Radioactive-Decay Gammas. At. Data Nucl. Data Tables 13 (1974) 89-292.

11) H. L. Beck, The Absolute Intensities of Gamma Rays from the Decay of ^{238}U and ^{232}Th. HASL-262 (1972) 14 pp.

12) E. K. Hyde, I. Perlman, and G. T. Seaborg, The Nuclear Properties of the Heavy Elements. Vol. 2 (Prentice-Hall, Englewood Cliffs, N. J., 1964) 1107 pp.

13) W. Jacobi and K. André, The Vertical Distribution of Radon 222, Radon 220 and Their Decay Products in the Atmosphere. J. Geophys. Res. 68 (1963) 3799-3814.

14) H. L. Beck, Gamma Radiation from Radon Daughters in the Atmosphere. J. Geophys. Res. 79 (1974) 2215-2221.

15) W. H. McMaster, N. Keer Del Grande, J. H. Mallett, and J. H. Hubbel, Compilation of X-Ray Cross Sections. UCRL-50174 (Sec. 1-4) (1969-70).

16) H. Goldstein, Fundamental Aspects of Reactor Shielding (Addison-Wesley, Reading, Mass., 1959) 416 pp.

17) A. Schaarschmidt and H.-J. Keller, Calculation of Efficiency and Cross Section of Cylindrical Scintillators in Axisymmetrical Gamma-Ray Fields. Nucl. Inst. Meth. 72 (1969) 82-92.

18) H.-J. Keller and A. Schaarschmidt, Empfindlichkeit und Wirkungsquerschnitt zylindrischer Szintillatoren in axial-symmetrischen Gamma-Strahlungsfeldern verschiedener Winkelverteilungen, BMwF-FB K-69-20 (1969) 125 pp.

19) F. H. Attix and W. C. Roesch, Radiation Dosimetry. 2nd edition, Vol. 1 (Academic Press, New York, 1968) 405 pp.

20) D. K. Trubey, A Table of Three Exponential Integrals, ORNL-2750 (1959) 63 pp.

21) J. S. Duval Jr., B. Cook, and J. A. S. Adams, Circle of Investigation of an Air-borne Gamma-Ray Spectrometer. J. Geophys. Res., 76 (1971) 8466-8470.

APPENDIX I

THE PLANE GAMMA-RAY TRANSPORT EQUATION FOR PURE COMPTON SCATTERERS

The plane, one-dimensional Boltzmann equation governing the transport of gamma rays through matter can be formulated as

$$\omega \frac{\partial}{\partial z} F(z, E, \omega) + \mu(z, E) F(z, E, \omega) = n_e(z) \int\int F(z, E', \omega') \sigma(E' \to E, \underline{\Omega}' \to \underline{\Omega}) \, d\underline{\Omega} dE' + \frac{q(z, E)}{4\pi} \quad (-\infty < z < \infty) \tag{A1}$$

where

$F(z, E, \omega)$	= angular gamma-ray flux ($\gamma \cdot cm^{-2} \cdot s^{-1} \cdot sterad^{-1}$)
z	= distance along the z-axis (cm)
E	= gamma-ray energy (MeV)
$\underline{\Omega}$	= unit vector in the direction of gamma-ray movement
ω	= $\underline{i} \cdot \underline{\Omega}$, where $\underline{i}$ is a unit vector parallel to the z-axis
$\mu(z, E)$	= total macroscopic cross section without coherent scattering (cm^{-1})
$n_e(z)$	= position distribution of electron density (electrons $\cdot$ cm^{-3})
$\sigma(E' \to E, \underline{\Omega}' \to \underline{\Omega})$	= microscopic transference cross section* for incoherent scattering from (E', $\underline{\Omega}'$) into (E, $\underline{\Omega}$) ($cm^2 \cdot MeV^{-1} \cdot sterad^{-1}$ per electron)
$q(z, E)$	= position and energy distribution of isotropically radiating source ($\gamma \cdot cm^{-3} \cdot MeV^{-1} \cdot s^{-1}$)

The double integral on the right-hand side of the formula is extended over all previous energies and directions.

We now suppose that the gamma-ray interactions are confined to the process of incoherent scattering, the macroscopic cross section $\mu(z, E)$ being taken as

---

* The transference cross section for incoherent scattering is derivable from Compton's and Klein-Nishina's formulas, cf. reference 1.

$$\mu(z, E) = n_e(z)\, \sigma_e(E)\,, \tag{A2}$$

where

$$\sigma_e(E) = \int\int \sigma(E \to E',\ \underline{\omega} \to \underline{\omega}')\, d\underline{\omega}'\, dE' \tag{A3}$$

is the incoherent-scattering cross section (cm^2 per electron) for a free electron. This implies that the material in the interval $-\infty < z < \infty$ is regarded as a cloud of electrons whose density varies according to $n_e(z)$. It is convenient to replace the distance z by the number of electrons per cm^2, ζ, in a column of the height z, i. e. we define

$$\zeta = \int_0^z n_e(z')dz'\,. \tag{A4}$$

With this new position variable the transport equation reads

$$\mu \frac{\partial}{\partial \zeta} F(\zeta, E, \underline{\omega}) + \sigma_e(E)\, F(\zeta, E, \underline{\omega}) = \int\int F(\zeta, E', \underline{\omega}')\, \sigma(E' \to E,\ \underline{\omega}' \to \underline{\omega})\, d\underline{\omega}'dE' + \frac{Q(\zeta, E)}{4\pi} \quad (-\infty < \zeta < \infty) \tag{A5}$$

where $Q(\zeta, E)$, the source density per electron, is given by

$$Q(\zeta, E) = \frac{q(z, E)}{n_e(z)}\,. \tag{A6}$$

APPENDIX II

THE EXPANSION COEFFICIENTS IN THE DOUBLE-P_l REPRESENTATION OF THE ANGULAR CHANNEL FLUX

In section 4.1 equations (11) we considered the double-P_l representation of the angular channel flux $\varphi(z, E, \omega)$:

$$\varphi(z, E, \omega) = \varphi^{+}(z, E, \omega) + \varphi^{-}(z, E, \omega) , \tag{A7}$$

and

$$\varphi^{\pm}(z, E, \omega) \approx \sum_{l=0}^{L} (2l+1)\, \varphi_l^{\pm}(z, E)\, P_l(2\omega^{\pm} - 1) , \tag{A8}$$

P_l being the Legendre polynomial of the order l. The expansion coefficients $\varphi_l^{\pm}(z, E)$ are given by [1]

$$\varphi_l^{\pm}(z, E) = \int^{\pm} \varphi^{\pm}(z, E, \omega)\, P_l(2\omega^{\pm} - 1)\, d\omega$$

$$(l = 0, 1; \int^{+} \equiv \int_0^1 \quad \text{and} \quad \int^{-} \equiv \int_{-1}^0) , \tag{A9}$$

and it is the objective of this appendix to discuss the evaluation of the right-hand side of (A9). In doing so, we first partition $\varphi^{\pm}(z, E, \omega)$ into an uncollided and a scattered part:

$$\varphi^{\pm}(z, E, \omega) = \varphi_u^{\pm}(z, E, \omega) + \varphi_s^{\pm}(z, E, \omega) \tag{A10}$$

and make a similar partitioning of the expansion coefficients:

$$\varphi_l^{\pm}(z, E) = \varphi_{l,u}^{\pm}(z, E) + \varphi_{l,s}^{\pm}(z, E) . \tag{A11}$$

$\varphi_{l,s}^{\pm}(z, E)$ are closely related to the expansion coefficients $\phi_l^{\pm}(z, \lambda)$ for the angular energy flux (i. e. energy x angular flux) discussed in 1) and available in the GAMMABANK data-file system (λ denotes the wavelength in Compton units, that is $\lambda = 0.511/E$). In fact, $\varphi_{l,s}^{\pm}$ results from a "channel integration", like that in equation (10), of $\phi_l^{\pm}(z, \lambda)$:

$$\varphi^{+}_{l,s}(z,E) = \int_{I(E)} \psi^{+}_{l}(z,\lambda')/E'dE' \,. \qquad (A12)$$

Here, the integration range I(E) is the channel interval corresponding to E (see section 4.1), and $\lambda' = 0.511/E'$. The numerical integration technique applied in evaluating (A12) is the same as used in the program GFX[1].

Next we turn to discuss the "uncollided" part of (A11), viz.

$$\varphi^{+}_{l,u}(z,E) = \int^{+} \varphi^{+}_{u}(z,E,\omega)\, P_l(2\omega^{+} - 1)\, d\omega. \qquad (A13)$$

As the "skyshine" does not include uncollided gamma rays, we have

$$\varphi^{-}_{l,u}(z,E) = 0, \qquad (A14)$$

and we need only consider the plus term

$$\varphi^{+}_{l,u}(z,E) = \int_{0}^{1} \varphi^{+}_{u}(z,E,\omega)\, P_l(2\omega - 1)\, d\omega. \qquad (A15)$$

$\varphi^{+}_{u}(z,E,\omega) = \varphi_u(z,E,\omega)$ is the angular channel flux of uncollided gamma rays; it is expressible as the following channel integral (cf. equation (4) in section 3.1):

$$\varphi_u(z,E,\omega) = \int_{I(E)} \sum_i u_i(z,\omega)\, \delta(E' - E_i)\, dE' \,, \qquad (A16)$$

or

$$\varphi_u(z,E,\omega) = \sum_{E_i \in I(E)} u_i(z,\omega) \,. \qquad (A17)$$

As indicated, the summation is restricted to source line energies belonging to the channel interval I(E); from (A15) we get

$$\varphi^{+}_{l,u}(z,E) = \sum_{E_i \in I(E)} \int_{0}^{1} u_i(z,\omega)\, P_l(2\omega - 1)\, d\omega \,. \qquad (A18)$$

Now, for $z \geq 0$ and $\omega > 0$ we have[1]

$$u_i(z,\omega) = \frac{q_i}{4\pi\,\mu_G(E_i)} \exp\left(-\frac{\mu_A(E_i)}{\omega}\, z\right). \tag{A19}$$

q_i is the source strength of line no i ($\gamma/cm^3\,s$)); $\mu_G(E_i)$ and $\mu_A(E_i)$ are the linear attenuation coefficients (cm^{-1}) in the ground and the air, respectively, taken at the line energy E_i. Restricting l to l = 0 and l = 1 and inserting $P_0(2\omega - 1) = 1$, $P_1(2\omega - 1) = 2\omega - 1$, we finally arrive at the expressions

$$\varphi^+_{0,u}(z,E) = \sum_{E_i \in I(E)} c_i\, E_2(x_i) \tag{A20}$$

and

$$\varphi^+_{1,u}(z,E) = \sum_{E_i \in I(E)} c_i\, [2\,E_3(x_i) - E_2(x_i)] \tag{A21}$$

with the abbreviations $c_i \equiv \frac{q_i}{4\pi\,\mu_G(E_i)}$ and $x_i \equiv \mu_A(E_i)z$. $E_n(x)$ stands for the nth-order exponential integral defined in equation (22), section 5.1. The term in brackets in (A21) can be equivalently expressed as

$$[\;] = \exp(-x_i) - (1 + x_i)\,E_2(x_i), \tag{A22}$$

so we shall only require an algorithm for the E_2-function.

Table I

Densities and compositions of the ground materials considered in this work

Oxide	Per cent abundance	
	Granite $\rho = 2.67\ g/cm^3$	Soil $\rho = 1.6\ g/cm^3$
SiO_2	70.18	67.5
TiO_2	0.39	
Al_2O_3	14.47	13.5
Fe_2O_3	1.57	4.5
FeO	1.78	
MnO	0.12	
MgO	0.88	
CaO	1.99	
Na_2O	3.48	
K_2O	4.11	
H_2O	0.84	10.0
CO_2		4.5
P_2O_5	0.19	

Table 2

Principal characteristics of the ^{232}Th decay chain

Isotope	Radiation	Half-life
^{232}Th	α	1.39×10^{10} y
^{228}Ra	β	5.75 y
^{228}Ac	β , γ	6.13 h
^{228}Th	α	1.91 y
^{224}Ra	α , γ	3.64 d
^{220}Rn	α	55.3 s
^{216}Po	α	0.15 s
^{212}Pb	β , γ	10.64 h
^{212}Bi	β γ(64%)	60.6 m
	α (36%)	
64%	36%	
^{212}Po	α	3×10^{-7} s
^{208}Tl	β, γ	3.1 m
^{208}Pb	stable	-

Table 3

Principal characteristics of the ^{238}U decay chain

Isotope	Radiation	Half-life
^{238}U	α	4.51×10^{9} y
^{234}Th	β	24.1 d
^{234}Pa	β	1.18 m
^{234}U	α , γ	2.48×10^{5} y
^{230}Th	α	8×10^{4} y
^{226}Ra	α , γ	1600 y
^{222}Rn	α	3.82 d
^{218}Po	α	3.05 m
^{214}Pb	β , γ	26.8 m
^{214}Bi	β , γ	19.8 m
^{214}Po	α	1.6×10^{-4} s
^{210}Pb	β , γ	21.3 y
^{210}Bi	β	5.01 d
^{210}Po	α	138.4 d
^{206}Pb	stable	-

Table 4

Dominant gamma-rays emitted by ^{232}Th daughters

Isotope	Gamma-ray energy (MeV)	Intensity (%)
^{212}Pb	0.2386	45.0
^{228}Ac	0.3385	12.3
^{208}Tl	0.5107	9.0
"	0.5831	30.0
^{212}Bi	0.7272	7.0
^{228}Ac	0.9111	29.0
"	0.9667	23.0
"	1.5881	4.6
^{208}Tl	2.6147	35.9

Table 5

Dominant gamma-rays emitted by ^{238}U daughters

Isotope	Gamma-ray energy (MeV)	Intensity (%)
^{214}Pb	0.2952	17.9
"	0.3520	35.0
^{214}Bi	0.6094	43.0
"	1.1204	14.5
"	1.2382	5.6
"	1.3778	4.6
"	1.7647	14.7
"	2.2045	4.7
"	2.4480	1.5

Table 6

Expansion coefficients $\varphi_0^+(z, E)$, $\varphi_1^+(z, E)$, $\varphi_0^-(z, E)$, and $\varphi_1^-(z, E)$ in $cm^{-2} \cdot s^{-1}$ to be used with the equations (11) for calculation of the energy and angular distribution of the natural gamma-ray flux above a ground (granite) with known abundances of thorium, uranium, and potassium. The expansion coefficients are given in 0.05 - MeV wide energy intervals for altitudes z of between 0 and 200 m in air having a density of 0.001293 g/cm^3.

	1 PPM THORIUM				1 PPM URANIUM				1% POTASSIUM			
E (MEV)	PH10•	PH11•	PH10•	PH11•	PH10•	PH11•	PH10•	PH11•	PH10•	PH11•	PH10•	PH11•
0.10•0.15	6.50E•03	2.54E•04	6.90E•03	3.01E•04	1.43E•02	5.81E•04	1.10E•02	6.64E•04	1.87E•02	6.53E•04	1.50E•02	7.81E•04
0.15•0.20	4.10E•03	2.03E•04	3.57E•03	2.13E•04	9.68E•03	4.24E•04	6.02E•03	4.66E•04	1.14E•02	3.42E•04	9.23E•03	5.68E•04
0.20•0.25	4.44E•03	1.96E•04	1.51E•03	1.40E•04	7.15E•03	3.05E•04	3.66E•03	3.93E•04	8.69E•03	2.10E•04	6.88E•03	2.19E•04
0.25•0.30	1.97E•03	1.25E•04	8.01E•04	1.26E•04	6.73E•03	3.54E•04	1.89E•03	3.57E•04	6.63E•03	3.03E•04	4.07E•03	3.48E•04
0.30•0.35	1.99E•03	1.11E•04	4.85E•04	1.12E•04	3.64E•03	2.78E•04	1.10E•03	2.79E•04	5.20E•03	4.01E•04	2.53E•03	4.03E•04
0.35•0.40	1.03E•03	9.62E•05	3.27E•04	9.65E•05	5.72E•03	2.09E•04	6.94E•04	2.05E•04	4.20E•03	3.93E•04	1.73E•03	3.94E•04
0.40•0.45	9.02E•04	8.48E•05	2.30E•04	8.42E•05	1.97E•03	1.80E•04	5.07E•04	1.81E•04	3.65E•03	3.45E•04	1.27E•03	3.66E•04
0.45•0.50	9.99E•04	7.10E•05	1.78E•04	7.11E•05	1.94E•03	1.57E•04	3.86E•04	1.57E•04	3.20E•03	3.33E•04	9.77E•04	3.33E•04
0.50•0.55	1.00E•03	5.83E•05	1.35E•04	5.84E•05	1.61E•03	1.33E•04	2.98E•04	1.33E•04	2.87E•03	3.01E•04	7.82E•04	3.01E•04
0.55•0.60	1.03E•03	4.63E•05	1.02E•04	4.64E•05	1.54E•03	1.07E•04	2.28E•04	1.08E•04	2.64E•03	2.72E•04	6.41E•04	2.72E•04
0.60•0.65	4.47E•04	3.90E•05	8.17E•05	3.91E•05	6.23E•03	7.55E•05	1.60E•04	7.56E•05	2.62E•03	2.40E•04	5.38E•04	2.46E•04
0.65•0.70	4.20E•04	3.40E•05	6.76E•05	3.40E•05	9.26E•04	6.48E•05	1.31E•04	6.49E•05	2.27E•03	2.23E•04	4.59E•04	2.23E•04
0.70•0.75	7.44E•04	2.87E•05	5.52E•05	2.87E•05	8.19E•04	5.48E•05	1.10E•04	5.48E•05	2.14E•03	2.01E•04	3.93E•04	2.01E•04
0.75•0.80	8.19E•04	2.37E•05	4.46E•05	2.37E•05	1.47E•03	4.90E•05	9.25E•05	4.91E•05	2.04E•03	1.83E•04	3.66E•04	1.83E•04
0.80•0.85	6.99E•04	1.96E•05	3.62E•05	1.97E•05	8.53E•04	4.31E•05	7.90E•05	4.32E•05	1.96E•03	1.66E•04	3.04E•04	1.66E•04
0.85•0.90	5.31E•04	1.59E•05	2.90E•05	1.59E•05	5.25E•04	3.83E•05	6.83E•05	3.84E•05	1.87E•03	1.50E•04	2.65E•04	1.50E•04
0.90•0.95	1.71E•03	1.19E•05	2.19E•05	1.19E•05	9.61E•04	3.37E•05	5.87E•05	3.37E•05	1.84E•03	1.36E•04	2.34E•04	1.36E•04
0.95•1.00	1.35E•03	9.21E•06	1.71E•05	9.24E•06	5.29E•04	2.96E•05	5.07E•05	2.97E•05	1.80E•03	1.23E•04	2.06E•04	1.23E•04
1.00•1.05	1.16E•04	8.19E•06	1.50E•05	8.22E•06	5.51E•04	2.60E•05	4.37E•05	2.60E•05	1.77E•03	1.11E•04	1.83E•04	1.11E•04
1.05•1.10	1.49E•04	7.51E•06	1.35E•05	7.54E•06	5.59E•04	2.21E•05	3.67E•05	2.22E•05	1.74E•03	9.90E•05	1.68E•04	9.91E•05
1.10•1.15	1.07E•04	6.90E•06	1.22E•05	6.93E•06	2.79E•03	1.80E•05	2.97E•05	1.80E•05	1.72E•03	8.80E•05	1.48E•04	8.81E•05
1.15•1.20	9.92E•05	6.40E•06	1.11E•05	6.43E•06	6.00E•04	1.57E•05	2.57E•05	1.57E•05	1.71E•03	7.79E•05	1.42E•04	7.79E•05
1.20•1.25	1.26E•04	5.90E•06	1.01E•05	5.93E•06	1.33E•03	1.35E•05	2.19E•05	1.36E•05	1.70E•03	6.68E•05	1.04E•04	6.69E•05
1.25•1.30	8.88E•05	5.45E•06	9.24E•06	5.46E•06	5.10E•04	1.18E•05	1.89E•05	1.18E•05	1.69E•03	5.66E•05	8.65E•05	5.65E•05
1.30•1.35	8.14E•05	5.03E•06	8.43E•06	5.06E•06	2.55E•04	1.03E•05	1.65E•05	1.04E•05	1.69E•03	4.56E•05	6.91E•05	4.57E•05
1.35•1.40	8.03E•05	4.62E•06	7.60E•06	4.65E•06	1.23E•03	8.69E•06	1.38E•05	8.72E•06	1.69E•03	3.52E•05	5.29E•05	3.53E•05
1.40•1.45	7.94E•05	4.21E•06	6.90E•06	4.24E•06	8.69E•04	7.91E•06	1.17E•05	7.93E•06	1.71E•03	1.49E•05	2.93E•05	1.49E•05
1.45•1.50	2.84E•04	3.81E•06	6.24E•06	3.84E•06	1.73E•04	4.54E•06	1.02E•05	4.56E•06	5.07E•02	5.16E•07	7.71E•07	5.18E•07
1.50•1.55	9.10E•05	3.41E•06	5.55E•06	3.43E•06	7.17E•04	5.63E•06	8.77E•06	5.65E•06				
1.55•1.60	4.46E•04	2.97E•06	4.84E•06	2.99E•06	4.27E•04	4.83E•06	7.48E•06	4.85E•06				
1.60•1.65	4.04E•04	2.70E•06	4.38E•06	2.72E•06	1.47E•04	4.07E•06	6.26E•06	4.08E•06				
1.65•1.70	7.34E•03	2.53E•06	4.08E•06	2.55E•06	4.01E•04	3.26E•06	5.03E•06	3.29E•06				
1.70•1.75	4.57E•03	2.38E•06	3.80E•06	2.40E•06	6.94E•04	2.40E•06	3.69E•06	2.42E•06				
1.75•1.80	4.58E•03	2.23E•06	3.55E•06	2.25E•06	3.12E•03	1.81E•06	2.69E•06	1.82E•06				
1.80•1.85	5.05E•03	2.09E•06	3.31E•06	2.11E•06	5.72E•04	1.27E•06	1.96E•06	1.28E•06				
1.85•1.90	5.12E•03	1.97E•06	3.09E•06	1.99E•06	1.48E•04	1.07E•06	1.64E•06	1.07E•06				
1.90•1.95	6.38E•03	1.84E•06	2.88E•06	1.86E•06	3.14E•05	9.34E•07	1.43E•06	9.62E•07				
1.95•2.00	4.35E•03	1.72E•06	2.68E•06	1.74E•06	3.13E•05	8.34E•07	1.27E•06	8.61E•07				
2.00•2.05	4.34E•03	1.60E•06	2.48E•06	1.62E•06	3.14E•05	7.31E•07	1.11E•06	7.37E•07				
2.05•2.10	4.31E•03	1.48E•06	2.30E•06	1.50E•06	3.15E•05	6.27E•07	9.49E•07	6.32E•07				
2.10•2.15	4.30E•03	1.38E•06	2.13E•06	1.40E•06	3.00E•04	5.27E•07	7.97E•07	5.32E•07				
2.15•2.20	4.29E•03	1.29E•06	1.98E•06	1.30E•06	2.64E•05	3.79E•07	5.72E•07	3.82E•07				
2.20•2.25	4.27E•03	1.20E•06	1.84E•06	1.21E•06	1.11E•03	2.36E•07	3.56E•07	2.38E•07				
2.25•2.30	4.27E•03	1.10E•06	1.68E•06	1.11E•06	8.77E•05	1.18E•07	1.78E•07	1.19E•07				
2.30•2.35	4.27E•03	9.79E•07	1.49E•06	9.92E•07	5.72E•06	7.10E•08	1.07E•07	7.18E•08				
2.35•2.40	4.27E•03	8.72E•07	1.33E•06	8.84E•07	5.75E•06	3.97E•08	5.99E•08	4.01E•08				
2.40•2.45	4.27E•03	7.49E•07	1.13E•06	7.59E•07	3.70E•04	1.20E•08	1.82E•08	1.22E•08				
2.45•2.50	4.30E•03	5.32E•07	8.05E•07	5.39E•07								
2.50•2.55	4.32E•03	3.23E•07	4.88E•07	3.27E•07								
2.55•2.60	4.34E•03	1.36E•07	2.06E•07	1.38E•07								
2.60•2.65	3.03E•03	7.47E•09	1.13E•08	7.57E•09								
SUM!	3.75E•02	1.40E•03	1.10E•02	1.54E•03	8.37E•02	3.34E•03	2.66E•02	3.48E•03	1.50E•01	5.64E•03	4.73E•02	5.81E•03

	1 PPM THORIUM				1 PPM URANIUM				1% POTASSIUM			
E (MEV)	PHI0+	PHI1+	PHI0-	PHI1-	PHI0+	PHI1+	PHI0-	PHI1-	PHI0+	PHI1+	PHI0-	PHI1-
0.10-0.15	6.40E-03	2.53E-04	4.85E-03	2.98E-04	1.43E-02	5.51E-04	1.09E-02	6.58E-04	1.87E-02	6.30E-04	1.55E-02	7.77E-04
0.15-0.20	4.08E-03	2.07E-04	2.54E-03	2.10E-04	9.60E-03	4.48E-04	5.95E-03	4.40E-04	1.14E-02	3.41E-04	9.17E-03	3.64E-04
0.20-0.25	4.32E-03	2.21E-04	1.49E-03	1.57E-04	7.07E-03	4.17E-04	3.42E-03	3.88E-04	8.55E-03	2.15E-04	6.81E-03	2.14E-04
0.25-0.30	1.95E-03	1.34E-04	7.92E-04	1.25E-04	6.58E-03	4.32E-04	1.86E-03	3.52E-04	6.60E-03	3.44E-04	4.04E-03	3.47E-04
0.30-0.35	1.94E-03	1.37E-04	4.79E-04	1.11E-04	3.62E-03	2.85E-04	1.09E-03	2.76E-04	5.10E-03	4.01E-04	2.59E-03	4.02E-04
0.35-0.40	1.03E-03	9.72E-05	3.23E-04	9.54E-05	5.49E-03	3.37E-04	6.85E-04	2.03E-04	4.26E-03	3.94E-04	1.72E-03	3.93E-04
0.40-0.45	9.73E-04	8.80E-05	2.34E-04	8.30E-05	1.96E-03	1.86E-04	5.00E-04	1.78E-04	3.64E-03	3.67E-04	1.26E-03	3.64E-04
0.45-0.50	9.84E-04	7.90E-05	1.75E-04	7.00E-05	1.83E-03	1.44E-04	3.79E-04	1.56E-04	3.19E-03	3.35E-04	9.68E-04	3.31E-04
0.50-0.55	1.05E-03	7.24E-05	1.33E-04	5.74E-05	1.60E-03	1.37E-04	2.92E-04	1.31E-04	2.80E-03	3.04E-04	7.72E-04	2.99E-04
0.55-0.60	1.76E-03	8.76E-05	1.00E-04	4.56E-05	1.53E-03	1.11E-04	2.23E-04	1.05E-04	2.61E-03	2.75E-04	6.32E-04	2.69E-04
0.60-0.65	4.44E-04	3.98E-05	8.01E-05	3.84E-05	5.96E-03	2.43E-04	1.57E-04	7.44E-05	2.41E-03	2.49E-04	5.27E-04	2.43E-04
0.65-0.70	4.27E-04	1.47E-05	6.61E-05	3.33E-05	9.13E-04	7.19E-05	1.29E-04	6.38E-05	2.20E-03	2.26E-04	4.51E-04	2.20E-04
0.70-0.75	7.45E-04	4.02E-05	5.39E-05	2.81E-05	8.10E-04	6.19E-05	1.08E-04	5.58E-05	2.13E-03	2.05E-04	3.88E-04	1.98E-04
0.75-0.80	7.96E-04	3.79E-05	4.36E-05	2.32E-05	1.42E-03	7.49E-05	9.05E-05	4.81E-05	2.03E-03	1.86E-04	3.37E-04	1.79E-04
0.80-0.85	4.89E-04	2.53E-05	3.54E-05	1.92E-05	8.38E-04	5.28E-05	7.73E-05	4.23E-05	1.90E-03	1.69E-04	2.95E-04	1.63E-04
0.85-0.90	5.19E-04	2.33E-05	2.83E-05	1.56E-05	5.24E-04	3.92E-05	6.67E-05	3.75E-05	1.89E-03	1.54E-04	2.59E-04	1.47E-04
0.90-0.95	1.64E-03	5.34E-05	2.15E-05	1.17E-05	9.39E-04	4.73E-05	5.73E-05	3.29E-05	1.84E-03	1.39E-04	2.28E-04	1.33E-04
0.95-1.00	1.29E-03	4.22E-05	1.60E-05	9.09E-06	5.25E-04	3.21E-05	4.93E-05	2.84E-05	1.79E-03	1.26E-04	2.01E-04	1.20E-04
1.00-1.05	1.15E-04	8.76E-06	1.47E-05	8.08E-06	5.45E-04	2.93E-05	4.25E-05	2.54E-05	1.76E-03	1.14E-04	1.77E-04	1.08E-04
1.05-1.10	1.47E-04	9.06E-06	1.33E-05	7.41E-06	5.53E-04	2.57E-05	3.57E-05	2.16E-05	1.74E-03	1.02E-04	1.55E-04	9.61E-05
1.10-1.15	1.06E-04	7.46E-06	1.20E-05	6.80E-06	2.69E-03	8.13E-05	2.89E-05	1.75E-05	1.72E-03	9.11E-05	1.36E-04	8.53E-05
1.15-1.20	9.85E-05	6.81E-06	1.09E-05	6.31E-06	5.48E-04	2.38E-05	2.50E-05	1.53E-05	1.71E-03	8.04E-05	1.17E-04	7.48E-05
1.20-1.25	1.24E-04	7.03E-06	9.92E-06	5.81E-06	1.29E-03	4.00E-05	2.13E-05	1.32E-05	1.69E-03	6.96E-05	9.98E-05	6.44E-05
1.25-1.30	8.84E-05	5.71E-06	9.04E-06	5.36E-06	4.99E-04	1.86E-05	1.84E-05	1.15E-05	1.69E-03	5.90E-05	8.35E-05	5.42E-05
1.30-1.35	8.12E-05	5.15E-06	8.25E-06	4.95E-06	2.54E-04	1.11E-05	1.60E-05	1.01E-05	1.69E-03	4.79E-05	6.80E-05	4.37E-05
1.35-1.40	8.01E-05	4.74E-06	7.50E-06	4.55E-06	1.20E-03	3.29E-05	1.34E-05	8.46E-06	1.69E-03	3.72E- 5	5.05E-05	3.37E-05
1.40-1.45	7.92E-05	4.32E-06	6.78E-06	4.14E-06	8.42E-04	2.42E-05	1.13E-05	7.21E-06	1.71E-03	1.80E 05	2.64E-05	1.62E-05
1.45-1.50	2.77E-04	8.76E-06	6.09E-06	3.75E-06	1.72E-04	6.77E-06	9.90E-06	6.35E-06	4.84E-02	1.18E-03	7.36E-07	4.94E-07
1.50-1.55	9.08E-05	3.94E-06	5.42E-06	3.35E-06	6.97E-04	1.86E-05	8.47E-06	5.47E-06				
1.55-1.60	4.33E-04	1.17E-05	4.73E-06	2.93E-06	4.17E-04	1.12E-05	7.22E-06	4.69E-06				
1.60-1.65	3.92E-04	1.08E-05	4.28E-06	2.66E-06	1.47E-04	4.23E-06	6.04E-06	3.94E-06				
1.65-1.70	7.23E-05	3.19E-06	3.98E-06	2.50E-06	3.91E-04	9.20E-06	4.84E-06	3.17E-06				
1.70-1.75	4.56E-05	2.44E-06	3.71E-06	2.34E-06	6.74E-04	1.50E-05	3.56E-06	2.33E-06				
1.75-1.80	4.49E-05	2.29E-06	3.46E-06	2.20E-06	3.01E-03	6.76E-05	2.40E-06	1.57E-06				
1.80-1.85	5.80E-05	2.45E-06	3.23E-06	2.06E-06	5.55E-04	1.26E-05	1.90E-06	1.24E-06				
1.85-1.90	5.09E-05	2.17E-06	3.01E-06	1.93E-06	1.45E-04	3.37E-06	1.59E-06	1.04E-06				
1.90-1.95	4.37E-05	1.89E-06	2.80E-06	1.81E-06	3.14E-05	9.69E-07	1.38E-06	9.11E-07				
1.95-2.00	4.34E-05	1.77E-06	2.61E-06	1.69E-06	3.13E-05	8.67E-07	1.23E-06	8.12E-07				
2.00-2.05	4.33E-05	1.65E-06	2.41E-06	1.57E-06	3.13E-05	7.60E-07	1.07E-06	7.11E-07				
2.05-2.10	4.31E-05	1.53E-06	2.23E-06	1.46E-06	3.14E-05	6.52E-07	9.17E-07	6.10E-07				
2.10-2.15	4.29E-05	1.43E-06	2.06E-06	1.36E-06	2.91E-04	6.05E-06	7.71E-07	5.14E-07				
2.15-2.20	4.28E-05	1.33E-06	1.92E-06	1.26E-06	2.64E-05	3.96E-07	5.54E-07	3.70E-07				
2.20-2.25	4.27E-05	1.24E-06	1.78E-06	1.18E-06	1.08E-03	2.19E-05	3.44E-07	2.30E-07				
2.25-2.30	4.26E-05	1.14E-06	1.63E-06	1.08E-06	8.59E-05	1.51E-06	1.72E-07	1.15E-07				
2.30-2.35	4.27E-05	1.01E-06	1.45E-06	9.62E-07	5.71E-06	7.40E-08	1.04E-07	6.94E-08				
2.35-2.40	4.27E-05	9.04E-07	1.28E-06	8.56E-07	5.79E-06	4.16E-08	5.80E-08	3.88E-08				
2.40-2.45	4.26E-05	7.78E-07	1.10E-06	7.35E-07	3.59E-04	7.00E-06	1.76E-08	1.18E-08				
2.45-2.50	4.30E-05	5.53E-07	7.79E-07	5.22E-07								
2.50-2.55	4.32E-05	3.37E-07	4.73E-07	3.16E-07								
2.55-2.60	4.34E-05	1.44E-07	1.99E-07	1.33E-07								
2.60-2.65	2.95E-03	5.65E-05	1.09E-08	7.33E-09								
SUM:	3.60E-02	1.05E-03	1.16E-02	1.52E-03	8.21E-02	4.17E-03	2.63E-02	3.43E-03	1.40E-01	6.88E-03	4.64E-02	5.74E-03

	1 PPM THORIUM				1 PPM URANIUM				1% POTASSIUM			
E (MEV)	PMI0*	PMI1*	PMI0*	PMI1*	PMI0*	PMI1*	PMI0*	PMI1*	PMI0*	PMI1*	PMI0*	PMI1*
0.10-0.15	5.72E-03	2.76E-04	3.94E-03	2.42E-04	1.20E-02	5.79E-04	8.93E-03	5.30E-04	1.77E-02	5.40E-04	1.33E-02	7.06E-04
0.15-0.20	3.63E-03	2.59E-04	2.01E-03	1.51E-04	7.09E-03	5.91E-04	4.00E-03	3.26E-04	1.02E-02	3.71E-04	7.92E-03	2.99E-04
0.20-0.25	3.04E-03	4.24E-04	1.15E-03	1.04E-04	5.60E-03	9.06E-04	2.63E-03	2.70E-04	7.37E-03	3.13E-04	5.70E-03	1.30E-04
0.25-0.30	1.59E-03	1.79E-04	6.16E-04	1.01E-04	4.88E-03	7.16E-04	1.39E-03	2.59E-04	5.70E-03	3.78E-04	3.38E-03	1.24E-04
0.30-0.35	1.44E-03	2.21E-04	3.65E-04	0.90E-05	3.05E-03	3.95E-04	7.98E-04	2.05E-04	4.59E-03	4.14E-04	2.03E-03	3.75E-04
0.35-0.40	0.97E-04	1.17E-04	2.39E-04	7.45E-05	3.40E-03	7.04E-04	5.00E-04	1.01E-04	3.81E-03	4.16E-04	1.38E-03	3.54E-04
0.40-0.45	0.32E-04	1.20E-04	1.66E-04	0.10E-05	1.40E-03	2.41E-04	3.55E-04	1.13E-04	3.27E-03	3.98E-04	9.88E-04	3.13E-04
0.45-0.50	7.90E-04	1.26E-04	1.20E-04	4.89E-05	1.55E-03	2.33E-04	2.56E-04	1.08E-04	2.87E-03	3.76E-04	7.04E-04	2.76E-04
0.50-0.55	7.67E-04	1.37E-04	0.81E-05	3.09E-05	1.38E-03	2.04E-04	1.89E-04	0.50E-05	2.57E-03	3.53E-04	5.74E-04	2.40E-04
0.55-0.60	1.13E-03	2.37E-04	4.63E-05	3.09E-05	1.31E-03	1.88E-04	1.40E-04	6.64E-05	2.35E-03	3.31E-04	4.50E-04	2.09E-04
0.60-0.65	3.93E-04	5.69E-05	9.19E-05	2.55E-05	3.52E-03	0.11E-04	1.05E-04	5.10E-05	2.17E-03	3.11E-04	3.73E-04	1.82E-04
0.65-0.70	3.75E-04	5.33E-05	4.12E-05	2.11E-05	7.49E-04	1.10E-04	0.44E-05	4.35E-05	2.03E-03	2.93E-04	3.08E-04	1.57E-04
0.70-0.75	9.43E-04	9.00E-05	3.27E-05	1.72E-05	6.77E-04	1.03E-04	6.09E-05	3.69E-05	1.91E-03	2.75E-04	2.50E-04	1.34E-04
0.75-0.80	5.60E-04	1.03E-04	2.61E-05	1.40E-05	1.00E-03	1.07E-04	5.66E-05	3.13E-05	1.84E-03	2.80E-04	2.10E-04	1.21E-04
0.80-0.85	3.77E-04	5.99E-05	2.10E-05	1.14E-05	0.53E-04	1.07E-04	4.73E-05	2.69E-05	1.75E-03	2.66E-04	1.83E-04	1.06E-04
0.85-0.90	3.05E-04	0.33E-05	1.60E-05	9.21E-06	6.65E-04	6.27E-05	3.96E-05	2.31E-05	1.68E-03	2.55E-04	1.55E-04	9.23E-05
0.90-0.95	1.02E-03	2.17E-04	1.35E-05	7.43E-06	7.00E-04	1.10E-04	3.33E-05	1.97E-05	1.64E-03	2.42E-04	1.32E-04	8.06E-05
0.95-1.00	0.06E-04	1.73E-04	1.12E-05	6.26E-06	6.49E-04	6.09E-05	2.79E-05	1.68E-05	1.59E-03	2.10E-04	1.13E-04	6.99E-05
1.00-1.05	1.00E-04	1.40E-05	9.80E-06	5.40E-06	6.50E-04	6.17E-05	2.35E-05	1.44E-05	1.57E-03	2.01E-04	9.83E-05	6.08E-05
1.05-1.10	1.10E-04	1.81E-05	8.77E-06	5.06E-06	6.59E-04	6.05E-05	1.95E-05	1.21E-05	1.54E-03	1.91E-04	8.16E-05	5.22E-05
1.10-1.15	9.10E-05	1.25E-05	7.00E-06	4.57E-06	1.73E-03	3.51E-04	1.61E-05	1.08E-05	1.52E-03	1.83E-04	6.87E-05	4.45E-05
1.15-1.20	0.65E-05	1.13E-05	7.01E-06	4.16E-06	4.44E-04	6.95E-05	1.37E-05	0.61E-06	1.51E-03	1.76E-04	5.72E-05	3.76E-05
1.20-1.25	1.02E-04	1.40E-05	6.20E-06	3.70E-06	0.77E-04	1.03E-04	1.16E-05	7.30E-06	1.49E-03	1.66E-04	4.65E-05	3.06E-05
1.25-1.30	7.00E-05	9.65E-06	5.64E-06	3.43E-06	3.70E-04	5.79E-05	9.89E-06	6.31E-06	1.47E-03	1.58E-04	3.66E-05	2.66E-05
1.30-1.35	7.10E-05	0.40E-06	5.00E-06	3.12E-06	2.22E-04	2.40E-05	0.66E-06	5.02E-06	1.46E-03	1.49E-04	2.78E-05	1.84E-05
1.35-1.40	7.20E-05	8.10E-06	4.56E-06	2.83E-06	0.10E-04	1.40E-04	7.07E-06	4.56E-06	1.44E-03	1.40E-04	1.64E-05	1.20E-05
1.40-1.45	7.30E-05	7.71E-06	4.09E-06	2.55E-06	9.79E-04	1.04E-04	5.96E-06	3.66E-06	1.50E-03	1.22E-04	7.51E-06	4.97E-06
1.45-1.50	1.97E-04	3.35E-05	3.66E-06	2.30E-06	1.55E-04	1.53E-05	5.11E-06	3.32E-06	3.12E-02	6.40E-03	2.34E-07	1.52E-07
1.50-1.55	7.77E-05	9.03E-06	3.26E-06	2.06E-06	6.09E-04	0.37E-05	4.31E-06	2.81E-06				
1.55-1.60	2.90E-04	5.35E-05	2.89E-06	1.83E-06	3.08E-04	4.70E-05	3.61E-06	2.37E-06				
1.60-1.65	2.67E-04	4.93E-05	2.62E-06	1.67E-06	1.32E-04	1.16E-05	2.90E-06	1.95E-06				
1.65-1.70	5.96E-05	7.77E-06	2.41E-06	1.55E-06	8.90E-04	4.29E-05	2.37E-06	1.55E-06				
1.70-1.75	6.19E-05	6.84E-06	2.22E-06	1.43E-06	6.73E-04	7.96E-05	1.76E-06	1.16E-06				
1.75-1.80	6.13E-05	6.00E-06	2.05E-06	1.33E-06	2.01E-03	3.01E-04	1.24E-06	0.13E-07				
1.80-1.85	6.90E-05	5.66E-06	1.89E-06	1.23E-06	3.79E-04	6.04E-05	9.08E-07	6.92E-07				
1.85-1.90	6.51E-05	6.60E-06	1.76E-06	1.14E-06	1.06E-04	1.61E-05	0.24E-07	5.66E-07				
1.90-1.95	6.02E-05	3.67E-06	1.59E-06	1.05E-06	2.06E-05	2.39E-06	7.09E-07	4.71E-07				
1.95-2.00	3.99E-05	3.95E-06	1.46E-06	9.63E-07	2.05E-05	2.29E-06	6.16E-07	4.11E-07				
2.00-2.05	3.90E-05	3.43E-06	1.33E-06	8.80E-07	2.06E-05	2.10E-06	5.20E-07	3.47E-07				
2.05-2.10	3.90E-05	3.32E-06	1.21E-06	0.04E-07	2.07E-05	2.07E-06	4.23E-07	2.82E-07				
2.10-2.15	3.93E-05	3.21E-06	1.10E-06	7.30E-07	2.05E-06	2.47E-05	3.34E-07	2.23E-07				
2.15-2.20	3.90E-05	3.11E-06	9.81E-07	6.54E-07	2.41E-05	1.56E-06	2.37E-07	1.58E-07				
2.20-2.25	3.93E-05	3.01E-06	0.75E-07	5.84E-07	7.40E-04	1.32E-04	1.47E-07	9.79E-08				
2.25-2.30	3.92E-05	2.90E-06	7.73E-07	5.18E-07	4.27E-05	9.32E-06	7.35E-08	4.89E-08				
2.30-2.35	3.94E-05	2.78E-06	6.71E-07	4.49E-07	5.35E-06	3.18E-07	4.02E-08	2.68E-08				
2.35-2.40	3.93E-05	2.67E-06	5.81E-07	3.87E-07	5.29E-06	2.02E-07	2.47E-08	1.64E-08				
2.40-2.45	3.93E-05	2.54E-06	4.85E-07	3.23E-07	2.50E-04	4.36E-05	7.68E-09	4.98E-09				
2.45-2.50	3.97E-05	2.30E-06	3.43E-07	2.28E-07								
2.50-2.55	0.00E-05	2.06E-06	2.08E-07	1.39E-07								
2.55-2.60	4.01E-05	1.80E-06	0.77E-08	5.04E-08								
2.60-2.65	2.07E-03	3.84E-04	4.03E-09	3.21E-09								
SUM*	2.00E-02	3.59E-03	9.07E-03	1.11E-03	6.38E-02	8.02E-03	2.05E-02	2.50E-03	1.20E-01	1.38E-02	3.00E-02	0.00E-03

Z = 90 N

	1 PPM THORIUM				1 PPM URANIUM				1% POTASSIUM			
E (MEV)	PHI0+	PHI1+	PHI0-	PHI1-	PHI0+	PHI1+	PHI0-	PHI1-	PHI0+	PHI1+	PHI0-	PHI1-
0.10-0.15	4.05E-03	3.11E-04	3.20E-03	1.97E-04	1.09E-02	6.67E-04	7.27E-03	4.30E-04	1.59E-02	6.61E-04	1.17E-02	6.29E-04
0.15-0.20	2.01E-03	2.70E-04	1.66E-03	1.09E-04	6.39E-03	6.07E-04	3.73E-03	2.43E-04	8.91E-03	4.09E-04	6.79E-03	2.43E-04
0.20-0.25	2.27E-03	3.95E-04	9.07E-04	7.21E-05	4.54E-03	5.91E-04	2.07E-03	2.02E-04	6.20E-03	3.45E-04	4.78E-03	8.16E-05
0.25-0.30	1.29E-03	1.70E-04	6.89E-04	8.10E-05	3.76E-03	6.90E-04	1.80E-03	1.97E-04	4.93E-03	3.63E-04	2.78E-03	2.94E-04
0.30-0.35	1.13E-03	2.08E-04	2.85E-04	7.17E-05	2.49E-03	4.33E-04	6.11E-04	1.58E-04	3.99E-03	4.04E-04	1.69E-03	3.37E-04
0.35-0.40	7.62E-04	1.22E-04	1.03E-04	5.07E-05	2.52E-03	6.17E-04	3.90E-04	1.20E-04	3.34E-03	4.89E-04	1.12E-03	3.10E-04
0.40-0.45	6.06E-04	1.20E-04	1.23E-04	4.62E-05	1.42E-03	2.55E-04	2.63E-04	1.02E-04	2.87E-03	4.00E-04	7.06E-04	2.69E-04
0.45-0.50	6.41E-04	1.34E-04	8.63E-05	3.59E-05	1.29E-03	2.55E-04	1.84E-04	7.93E-05	2.53E-03	3.87E-04	5.78E-04	2.29E-04
0.50-0.55	6.17E-04	1.44E-04	6.83E-05	2.79E-05	1.15E-03	2.37E-04	1.31E-04	6.67E-05	2.27E-03	3.72E-04	4.39E-04	1.94E-04
0.55-0.60	8.10E-04	2.20E-04	6.65E-05	2.21E-05	1.07E-03	2.34E-04	9.51E-05	4.60E-05	2.06E-03	3.57E-04	3.42E-04	1.66E-04
0.60-0.65	3.35E-04	6.69E-05	3.50E-05	1.79E-05	2.30E-03	7.50E-04	7.34E-05	3.74E-05	1.90E-03	3.43E-04	2.71E-04	1.39E-04
0.65-0.70	3.17E-04	6.53E-05	2.77E-05	1.43E-05	6.22E-04	1.32E-04	5.02E-05	3.12E-05	1.70E-03	3.30E-04	2.16E-04	1.16E-04
0.70-0.75	4.10E-04	1.05E-04	2.16E-05	1.15E-05	5.65E-04	1.19E-04	4.63E-05	2.59E-05	1.67E-03	3.17E-04	1.77E-04	1.00E-04
0.75-0.80	4.22E-04	1.10E-04	1.70E-05	9.28E-06	7.65E-04	1.95E-04	3.75E-05	2.16E-05	1.59E-03	3.07E-04	1.45E-04	8.54E-05
0.80-0.85	2.90E-04	7.06E-05	1.36E-05	7.51E-06	5.20E-04	1.20E-04	3.07E-05	1.83E-05	1.52E-03	2.98E-04	1.20E-04	7.29E-05
0.85-0.90	2.97E-04	7.34E-05	1.09E-05	6.00E-06	3.99E-04	8.00E-05	2.52E-05	1.53E-05	1.46E-03	2.88E-04	9.92E-05	6.20E-05
0.90-0.95	7.12E-04	2.15E-04	9.09E-06	5.13E-06	5.50E-04	1.33E-04	2.09E-05	1.29E-05	1.41E-03	2.81E-04	8.20E-05	5.27E-05
0.95-1.00	5.44E-04	1.70E-04	7.02E-06	4.51E-06	3.76E-04	7.84E-05	1.72E-05	1.08E-05	1.37E-03	2.74E-04	6.85E-05	4.44E-05
1.00-1.05	8.67E-05	1.66E-05	6.86E-06	4.04E-06	3.79E-04	8.04E-05	1.43E-05	9.02E-06	1.34E-03	2.69E-04	5.69E-05	3.74E-05
1.05-1.10	9.80E-05	2.07E-05	6.02E-06	3.61E-06	3.77E-04	8.03E-05	1.18E-05	7.46E-06	1.31E-03	2.63E-04	4.45E-05	3.09E-05
1.10-1.15	7.93E-05	1.52E-05	5.30E-06	3.22E-06	1.24E-03	3.59E-04	9.74E-06	6.25E-06	1.29E-03	2.58E-04	3.75E-05	2.51E-05
1.15-1.20	7.52E-05	1.41E-05	4.72E-06	2.90E-06	3.50E-04	8.19E-05	8.20E-06	5.29E-06	1.27E-03	2.55E-04	2.95E-05	1.98E-05
1.20-1.25	8.54E-05	1.75E-05	4.19E-06	2.60E-06	6.49E-04	1.75E-04	6.07E-06	4.45E-06	1.25E-03	2.50E-04	2.23E-05	1.51E-05
1.25-1.30	6.88E-05	1.26E-05	3.73E-06	2.34E-06	2.99E-04	6.91E-05	5.77E-06	3.76E-06	1.24E-03	2.46E-04	1.81E-05	1.09E-05
1.30-1.35	6.50E-05	1.15E-05	3.33E-06	2.10E-06	1.08E-04	3.59E-05	4.83E-06	3.16E-06	1.23E-03	2.42E-04	1.07E-05	7.22E-06
1.35-1.40	6.39E-05	1.12E-05	2.97E-06	1.89E-06	6.06E-04	1.61E-04	4.01E-06	2.63E-06	1.23E-03	2.38E-04	6.94E-06	3.31E-06
1.40-1.45	6.29E-05	1.10E-05	2.65E-06	1.69E-06	4.33E-04	1.14E-04	3.34E-06	2.20E-06	1.23E-03	2.28E-04	1.26E-06	8.29E-07
1.45-1.50	1.51E-04	3.73E-05	2.36E-06	1.51E-06	1.32E-04	2.37E-05	2.78E-06	1.84E-06	2.22E-02	6.56E-03	3.89E-08	2.53E-08
1.50-1.55	6.59E-05	1.22E-05	2.10E-06	1.35E-06	3.70E-04	9.39E-05	2.29E-06	1.52E-06				
1.55-1.60	2.23E-04	5.81E-05	1.87E-06	1.22E-06	2.40E-04	5.61E-05	1.86E-06	1.23E-06				
1.60-1.65	2.00E-04	5.20E-05	1.69E-06	1.11E-06	1.12E-04	1.94E-05	1.49E-06	9.85E-07				
1.65-1.70	5.02E-05	9.69E-06	1.54E-06	1.01E-06	2.26E-04	5.20E-05	1.16E-06	7.64E-07				
1.70-1.75	3.73E-05	6.03E-06	1.40E-06	9.25E-07	3.57E-04	9.00E-05	8.78E-07	5.81E-07				
1.75-1.80	3.67E-05	5.80E-06	1.28E-06	8.45E-07	1.47E-03	4.07E-04	4.51E-07	4.33E-07				
1.80-1.85	4.20E-05	7.59E-06	1.16E-06	7.69E-07	2.03E-04	7.47E-05	5.27E-07	3.51E-07				
1.85-1.90	3.92E-05	6.50E-06	1.05E-06	7.00E-07	8.30E-05	1.91E-05	4.37E-07	2.93E-07				
1.90-1.95	3.35E-05	5.35E-06	9.51E-07	6.33E-07	2.40E-05	3.93E-06	3.66E-07	2.45E-07				
1.95-2.00	3.53E-05	5.45E-06	8.58E-07	5.72E-07	2.47E-05	3.87E-06	3.06E-07	2.05E-07				
2.00-2.05	3.51E-05	5.37E-06	7.66E-07	5.12E-07	2.47E-05	3.80E-06	2.42E-07	1.63E-07				
2.05-2.10	3.49E-05	5.28E-06	6.[illegible]E-07	4.50E-07	2.40E-05	3.73E-06	1.77E-07	1.19E-07				
2.10-2.15	3.47E-05	5.20E-06	5.[illegible]E-07	4.02E-07	1.55E-04	3.90E-05	1.22E-07	8.14E-08				
2.15-2.20	3.47E-05	5.13E-06	5.04E-07	3.41E-07	2.08E-05	2.98E-06	8.28E-08	5.53E-08				
2.20-2.25	3.45E-05	5.06E-06	4.20E-07	2.86E-07	5.50E-05	1.45E-06	5.10E-08	3.19E-08				
2.25-2.30	3.44E-05	4.98E-06	3.44E-07	2.37E-07	4.09E-05	1.11E-05	2.49E-08	1.64E-08				
2.30-2.35	3.45E-05	4.91E-06	2.83E-07	1.92E-07	4.55E-06	6.25E-07	1.49E-08	9.78E-09				
2.35-2.40	3.44E-05	4.83E-06	2.36E-07	1.51E-07	4.57E-06	6.01E-07	8.31E-09	5.47E-09				
2.40-2.45	3.44E-05	4.73E-06	1.74E-07	1.15E-07	1.70E-04	4.85E-05	2.52E-09	1.66E-09				
2.45-2.50	3.44E-05	4.56E-06	1.22E-07	8.04E-08								
2.50-2.55	3.48E-05	4.39E-06	7.41E-08	4.88E-08								
2.55-2.60	3.48E-05	4.24E-06	3.12E-08	2.06E-08								
2.60-2.65	1.58E-03	3.99E-04	1.72E-09	1.13E-09								
SUM=	2.28E-02	3.79E-03	7.19E-03	8.35E-04	5.06E-02	8.45E-03	1.62E-02	1.88E-03	9.94E-02	1.54E-02	3.24E-02	1.57E-03

E (MEV)	1 PPM THORIUM				1 PPM URANIUM				1% POTASSIUM			
	PH10+	PH11+	PH10-	PH11-	PH10+	PH11+	PH10-	PH11-	PH10+	PH11+	PH10-	PH11-
0.10-0.15	4.06E-03	3.10E-04	2.61E-03	1.02E-04	9.15E-03	6.75E-04	5.94E-03	3.61E-04	1.44E-02	7.10E-04	1.01E-02	5.57E-04
0.15-0.20	2.29E-03	2.50E-04	1.31E-03	8.03E-05	5.10E-03	5.56E-04	3.01E-03	1.64E-04	7.73E-03	6.12E-04	5.03E-03	1.97E-04
0.20-0.25	1.75E-03	3.30E-04	7.37E-04	5.36E-05	3.64E-03	5.32E-04	1.67E-03	1.51E-04	5.35E-03	3.69E-04	4.05E-03	5.69E-05
0.25-0.30	1.06E-03	1.61E-04	3.98E-04	6.58E-05	2.95E-03	5.99E-04	8.66E-04	1.50E-04	4.22E-03	3.04E-04	2.33E-03	2.02E-04
0.30-0.35	9.02E-04	1.81E-04	2.30E-04	5.80E-05	2.03E-03	4.09E-04	4.88E-04	1.28E-04	3.44E-03	3.79E-04	1.41E-03	2.90E-04
0.35-0.40	6.42E-04	1.14E-04	1.46E-04	4.74E-05	1.91E-03	5.01E-04	3.09E-04	1.08E-04	2.90E-03	3.88E-04	9.22E-04	2.69E-04
0.40-0.45	5.72E-04	1.22E-04	9.65E-05	3.66E-05	1.19E-03	2.45E-04	2.05E-04	8.09E-05	2.50E-03	3.81E-04	6.49E-04	2.27E-04
0.45-0.50	5.25E-04	1.20E-04	6.65E-05	2.80E-05	1.07E-03	2.44E-04	1.41E-04	6.18E-05	2.21E-03	3.75E-04	4.63E-04	1.91E-04
0.50-0.55	4.94E-04	1.35E-04	4.74E-05	2.15E-05	9.56E-04	2.37E-04	9.88E-05	4.67E-05	1.98E-03	3.66E-04	3.43E-04	1.59E-04
0.55-0.60	4.87E-04	1.99E-04	3.50E-05	1.69E-05	8.81E-04	2.41E-04	7.10E-05	3.53E-05	1.80E-03	3.57E-04	2.64E-04	1.32E-04
0.60-0.65	2.05E-04	6.90E-05	2.60E-05	1.36E-05	1.70E-03	6.26E-04	5.47E-05	2.68E-05	1.66E-03	3.48E-04	2.05E-04	1.09E-04
0.65-0.70	2.60E-04	6.86E-05	2.03E-05	1.07E-05	5.22E-04	1.32E-04	4.28E-05	2.17E-05	1.55E-03	3.39E-04	1.62E-04	9.10E-05
0.70-0.75	3.31E-04	1.01E-04	1.57E-05	8.49E-06	4.75E-04	1.22E-04	3.34E-05	1.74E-05	1.45E-03	3.31E-04	1.24E-04	7.50E-05
0.75-0.80	3.29E-04	1.04E-04	1.23E-05	6.86E-06	6.02E-04	1.83E-04	2.66E-05	1.40E-05	1.37E-03	3.23E-04	1.03E-04	6.31E-05
0.80-0.85	3.40E-04	7.15E-05	9.81E-06	5.56E-06	4.34E-04	1.20E-04	2.15E-05	1.13E-05	1.31E-03	3.18E-04	8.31E-05	5.27E-05
0.85-0.90	2.36E-04	7.31E-05	7.91E-06	4.49E-06	3.41E-04	8.73E-05	1.73E-05	1.09E-05	1.26E-03	3.12E-04	6.72E-05	4.37E-05
0.90-0.95	5.19E-04	1.89E-04	6.64E-06	3.86E-06	4.42E-04	1.31E-04	1.41E-05	9.03E-06	1.21E-03	3.08E-04	5.43E-05	3.61E-05
0.95-1.00	4.13E-04	1.69E-04	5.74E-06	3.43E-06	3.17E-04	8.55E-05	1.14E-05	7.39E-06	1.17E-03	3.03E-04	4.36E-05	2.99E-05
1.00-1.05	7.54E-05	1.70E-05	9.00E-06	3.05E-06	3.16E-04	8.76E-05	9.25E-06	6.03E-06	1.14E-03	3.00E-04	3.43E-05	2.36E-05
1.05-1.10	8.27E-05	2.12E-05	6.35E-06	2.70E-06	3.12E-04	8.81E-05	7.46E-06	4.68E-06	1.11E-03	2.97E-04	2.66E-05	1.80E-05
1.10-1.15	6.80E-05	1.65E-05	3.79E-06	2.39E-06	9.19E-04	1.24E-04	6.16E-06	4.09E-06	1.07E-03	2.95E-04	1.98E-05	1.34E-05
1.15-1.20	6.54E-05	1.56E-05	3.34E-06	2.13E-06	2.82E-04	6.37E-05	5.06E-06	3.37E-06	1.07E-03	2.93E-04	1.63E-05	1.01E-05
1.20-1.25	7.24E-05	1.85E-05	2.94E-06	1.89E-06	4.97E-04	1.05E-04	4.14E-06	2.77E-06	1.06E-03	2.91E-04	9.81E-06	8.94E-06
1.25-1.30	5.99E-05	1.42E-05	2.60E-06	1.66E-06	2.41E-04	7.12E-05	3.39E-06	2.28E-06	1.04E-03	2.90E-04	8.26E-06	6.40E-06
1.30-1.35	5.68E-05	1.33E-05	2.29E-06	1.49E-06	1.59E-04	4.18E-05	2.73E-06	1.84E-06	1.03E-03	2.88E-04	3.69E-06	2.44E-06
1.35-1.40	5.57E-05	1.31E-05	2.02E-06	1.32E-06	4.45E-04	1.53E-04	2.23E-06	1.51E-06	1.02E-03	2.88E-04	4.29E-07	3.13E-07
1.40-1.45	5.47E-05	1.30E-05	1.78E-06	1.16E-06	3.34E-04	1.09E-04	1.82E-06	1.24E-06	1.02E-03	2.82E-04	*5.67E-07	*3.95E-07
1.45-1.50	1.20E-04	3.66E-05	1.57E-06	1.03E-06	1.13E-04	2.86E-05	1.45E-06	9.86E-07	1.64E-02	5.89E-03	*1.73E-06	*1.17E-06
1.50-1.55	5.62E-05	1.39E-05	1.39E-06	9.18E-07	2.09E-04	9.17E-05	1.15E-06	7.88E-07				
1.55-1.60	1.73E-04	5.54E-05	1.24E-06	8.30E-07	1.92E-04	5.74E-05	8.90E-07	6.01E-07				
1.60-1.65	1.55E-04	4.98E-05	1.11E-06	7.48E-07	9.56E-05	2.39E-05	6.77E-07	4.55E-07				
1.65-1.70	4.27E-05	1.06E-05	9.99E-07	6.73E-07	1.80E-04	5.36E-05	5.06E-07	3.38E-07				
1.70-1.75	3.29E-05	7.24E-06	8.93E-07	6.03E-07	2.78E-04	8.80E-05	3.96E-07	2.65E-07				
1.75-1.80	3.23E-05	7.11E-06	7.97E-07	5.40E-07	1.12E-03	3.78E-04	3.18E-07	2.15E-07				
1.80-1.85	3.68E-05	8.70E-06	7.08E-07	4.81E-07	2.19E-04	7.11E-05	2.61E-07	1.78E-07				
1.85-1.90	3.41E-05	7.79E-06	6.27E-07	4.27E-07	6.65E-05	1.95E-05	2.14E-07	1.46E-07				
1.90-1.95	3.12E-05	6.85E-06	5.52E-07	3.76E-07	2.15E-05	4.95E-06	1.72E-07	1.18E-07				
1.95-2.00	3.09E-05	6.77E-06	4.85E-07	3.31E-07	2.14E-05	4.91E-06	1.36E-07	9.25E-08				
2.00-2.05	3.08E-05	6.72E-06	4.21E-07	2.87E-07	2.13E-05	4.87E-06	9.78E-08	6.68E-08				
2.05-2.10	3.06E-05	6.66E-06	3.63E-07	2.48E-07	2.13E-05	4.83E-06	5.99E-08	4.11E-08				
2.10-2.15	3.04E-05	6.60E-06	3.08E-07	2.10E-07	1.22E-04	3.80E-05	2.69E-08	2.00E-08				
2.15-2.20	3.03E-05	6.56E-06	2.49E-07	1.71E-07	1.79E-05	3.95E-06	1.69E-08	1.17E-08				
2.20-2.25	3.01E-05	6.50E-06	1.98E-07	1.37E-07	4.33E-04	1.39E-04	9.75E-09	6.63E-09				
2.25-2.30	3.00E-05	6.45E-06	1.50E-07	1.04E-07	3.91E-05	1.13E-05	3.96E-09	2.54E-09				
2.30-2.35	3.00E-05	6.41E-06	1.06E-07	7.25E-08	3.92E-06	8.39E-07	2.18E-09	1.36E-09				
2.35-2.40	2.99E-05	6.35E-06	6.60E-08	4.43E-08	3.93E-06	8.24E-07	1.22E-09	7.59E-10				
2.40-2.45	2.98E-05	6.28E-06	3.48E-08	2.22E-08	1.49E-04	4.67E-05	3.69E-10	2.30E-10				
2.45-2.50	3.00E-05	6.18E-06	2.29E-08	1.45E-08								
2.50-2.55	3.01E-05	6.08E-06	1.39E-08	8.78E-09								
2.55-2.60	3.61E-05	5.97E-06	5.85E-09	3.70E-09								
2.60-2.65	1.24E-03	3.06E-04	3.22E-10	2.03E-10								
SUM+	1.85E-02	3.57E-03	5.82E-03	6.93E-04	4.07E-02	7.93E-03	1.31E-02	1.47E-03	8.13E-02	1.52E-02	2.73E-02	2.93E-03

Z = 100 M

	1 PPM THORIUM				1 PPM URANIUM				1% POTASSIUM			
E (MEV)	PM10*	PM11*	PM10*	PM11*	PM10*	PM11*	PM10*	PM11*	PM10*	PM11*	PM10*	PM11*
0.10-0.15	3.40E-03	2.07E-04	2.14E-03	1.34E-04	7.65L-03	4.32E-04	4.86L-03	2.99L-04	1.25L-02	7.23L-04	8.71E-03	4.99L-04
0.15-0.20	1.86E-03	2.16E-04	1.00E-03	6.07E-05	4.21E-03	4.79L-04	2.67L-03	1.63L-04	6.67L-03	3.91L-04	5.00E-03	1.83L-04
0.20-0.25	1.37E-03	2.63E-04	6.11E-04	4.20E-05	2.94L-03	4.53E-04	1.37L-03	1.15E-04	4.57L-03	3.47L-04	3.44E-03	4.42L-05
0.25-0.30	8.69E-04	1.30E-04	3.30E-04	5.41E-05	2.35L-03	4.99L-04	7.13E-04	1.47L-04	3.61L-03	3.30E-04	1.97L-03	2.32L-05
0.30-0.35	7.31E-04	1.91E-04	1.90E-04	4.85E-05	1.66L-03	3.57E-04	4.02L-04	1.07E-04	2.94L-03	3.62E-04	1.18E-03	2.61L-05
0.35-0.40	5.41E-04	1.05E-04	1.19E-04	3.90E-05	1.49L-03	4.00L-04	2.52L-04	8.60L-05	2.51L-03	3.50E-04	7.60E-04	2.33L-05
0.40-0.45	4.70E-04	1.11E-04	7.84E-05	3.00E-05	1.00L-03	2.43L-04	1.65L-04	6.63L-05	2.17L-03	3.52E-04	5.27E-04	1.95L-05
0.45-0.50	4.34E-04	1.16E-04	5.37E-05	2.29E-05	8.98L-04	2.47E-04	1.12E-04	5.04L-05	1.94L-03	3.51E-04	3.77E-04	1.61L-05
0.50-0.55	4.02E-04	1.19E-04	3.80E-05	1.76E-05	8.00L-04	2.22L-04	7.85L-05	3.60L-05	1.73L-03	3.46L-04	2.77E-04	1.32L-05
0.55-0.60	4.48E-04	1.66E-04	2.70E-05	1.37E-05	7.34L-04	2.45E-04	5.62L-05	2.88L-05	1.57L-03	3.41E-04	2.06E-04	1.08L-05
0.60-0.65	2.43E-04	6.62E-05	2.09E-05	1.09E-05	1.29E-03	5.92E-04	4.27L-05	2.31L-05	1.45E-03	3.38E-04	1.63E-04	8.77L-06
0.65-0.70	2.27E-04	6.63E-05	1.50E-05	8.56E-06	6.41E-04	1.24L-04	3.30L-05	1.87L-05	1.35E-03	3.30E-04	1.24E-04	7.17L-06
0.70-0.75	2.67E-04	9.12E-05	1.22E-05	6.75E-06	4.02E-04	1.17E-04	2.50L-05	1.51L-05	1.28E-03	3.42L-04	9.67E-05	5.86L-06
0.75-0.80	2.62E-04	9.35E-05	9.56E-06	5.43E-06	4.65L-04	1.04L-04	1.99L-05	1.23L-05	1.17L-03	3.20L-04	7.59E-05	4.79L-06
0.80-0.85	1.97E-04	6.70E-05	7.57E-06	4.39E-06	3.02E-04	1.13E-04	1.58L-05	1.00L-05	1.19L-03	3.18E-04	5.99E-05	3.91L-06
0.85-0.90	1.91E-04	6.77E-05	6.10E-06	3.58E-06	2.93E-04	8.72L-05	1.24L-05	8.10L-06	1.09L-03	3.12E-04	4.69E-05	3.15E-06
0.90-0.95	3.90E-04	1.40E-04	5.11E-06	3.06E-06	3.62E-04	1.23E-04	9.86L-06	6.55L-06	1.03L-03	3.07L-04	3.63L-05	2.50L-06
0.95-1.00	3.11E-04	1.25E-04	4.40E-06	2.71E-06	2.69E-04	8.51E-05	7.73E-06	5.20L-06	1.01E-03	3.06L-04	2.76E-05	1.94L-06
1.00-1.05	6.50E-05	1.70E-05	3.79E-06	2.39L-06	2.07E-04	8.09E-05	6.04L-06	4.10L-06	9.80L-04	3.05L-04	2.09E-05	1.67E-06
1.05-1.10	7.07E-05	2.07E-05	3.26E-06	2.09E-06	2.62E-04	8.75L-05	4.73E-06	3.22L-06	9.54E-04	3.03E-04	1.44E-05	1.07L-06
1.10-1.15	6.00E-05	1.67E-05	2.81E-06	1.83E-06	7.02E-04	2.41L-04	3.86L-06	2.69E-06	9.33L-04	3.02E-04	9.82E-06	7.69L-06
1.15-1.20	5.71E-05	1.59E-05	2.45E-06	1.61E-06	2.32E-04	8.00E-05	3.07L-06	2.14L-06	9.13L-04	3.01E-04	6.91E-06	5.73L-06
1.20-1.25	8.38E-05	1.84E-05	2.12E-06	1.41E-06	3.91L-04	1.48E-04	2.63L-06	1.71L-06	8.96L-04	3.00E-04	3.92E-06	2.98L-06
1.25-1.30	5.25E-05	1.48E-05	1.84E-06	1.23E-06	1.98L-04	6.84E-05	1.91E-06	1.38L-06	8.82L-04	3.00E-04	2.17E-06	1.68L-06
1.30-1.35	4.99E-05	1.40E-05	1.60E-06	1.07E-06	1.36E-04	4.34L-05	1.47E-06	1.09L-06	8.73L-04	3.00E-04	1.91E-06	1.38L-06
1.35-1.40	4.88E-05	1.39E-05	1.38E-06	9.31E-07	3.66E-04	1.39L-04	1.18L-06	8.39L-07	8.63L-04	3.00E-04	*8.88E-07	*8.81E-07
1.40-1.45	4.79E-05	1.38E-05	1.20E-06	8.09E-07	2.66L-04	9.87E-05	9.35L-07	6.67L-07	8.54L-04	3.00E-04	*8.67E-07	*5.76L-07
1.45-1.50	9.70E-05	3.40E-05	1.04E-06	7.05E-07	9.75L-05	3.04E-05	7.06L-07	5.01L-07	1.24L-02	5.07E-03	*2.65E-08	*1.76L-08
1.50-1.55	4.06E-05	1.45E-05	9.10E-07	6.22E-07	2.30E-04	8.46E-05	5.34L-07	3.76L-07				
1.55-1.60	1.37E-04	5.04E-05	8.16E-07	5.64E-07	1.56L-04	5.50E-05	3.92L-07	2.73L-07				
1.60-1.65	1.23E-04	4.49E-05	7.23E-07	5.03E-07	8.22L-05	2.50E-05	2.81L-07	1.93L-07				
1.65-1.70	3.67E-05	1.00E-05	6.36E-07	4.43E-07	1.47L-04	5.16L-05	2.01L-07	1.37L-07				
1.70-1.75	2.91E-05	7.88E-06	5.53E-07	3.87E-07	2.21L-04	8.13E-05	1.66L-07	1.12L-07				
1.75-1.80	2.66E-05	7.76E-06	4.80E-07	3.36L-07	8.69E-04	3.45L-04	1.46L-07	9.98L-08				
1.80-1.85	3.20E-05	9.17E-06	4.15E-07	2.92E-07	1.73E-04	6.63E-05	1.20E-07	8.17L-08				
1.85-1.90	2.98E-05	8.37E-06	3.57E-07	2.52E-07	5.42E-05	1.87L-05	9.66L-08	6.47L-08				
1.90-1.95	2.75E-05	7.94E-06	3.05E-07	2.15E-07	1.87E-05	5.45E-06	7.45L-08	5.23L-08				
1.95-2.00	2.73E-05	7.48E-06	2.59E-07	1.82L-07	1.86L-05	5.42E-06	5.46L-08	3.82L-08				
2.00-2.05	2.71E-05	7.45E-06	2.17E-07	1.53E-07	1.85L-05	5.40E-06	3.31L-08	2.33L-08				
2.05-2.10	2.69E-05	7.40E-06	1.80E-07	1.27E-07	1.85L-05	5.39L-06	1.07L-08	8.28L-09				
2.10-2.15	2.67E-05	7.36E-06	1.48E-07	1.03E-07	9.75L-05	3.51E-05	*6.91L-09	*3.45L-09				
2.15-2.20	2.66E-05	7.33E-06	1.18E-07	8.23E-08	1.55L-05	4.47E-06	*7.99L-09	*6.72L-09				
2.20-2.25	2.64E-05	7.29E-06	9.11E-08	6.36E-08	3.43L-04	1.26L-04	*5.80L-09	*3.86L-09				
2.25-2.30	2.63E-05	7.26E-06	6.20E-08	4.35E-08	3.10L-05	1.08L-05	*3.92L-09	*2.66L-09				
2.30-2.35	2.63E-05	7.24E-06	3.87E-08	2.02E-08	3.41L-06	9.57E-07	*2.56L-09	*1.77L-09				
2.35-2.40	2.62E-05	7.21E-06	*9.56E-10	*2.40E-10	3.41L-06	9.50L-07	*1.64L-09	*9.10L-10				
2.40-2.45	2.61E-05	7.19E-06	*2.09E-08	*1.45L-08	1.19L-04	4.24L-05	*6.38L-10	*1.10L-10				
2.45-2.50	2.61E-05	7.11E-06	*1.65E-06	*1.15E-08								
2.50-2.55	2.62E-05	7.06E-06	*1.00E-08	*6.95E-09								
2.55-2.60	2.61E-05	7.00E-06	*6.23E-09	*2.63E-09								
2.60-2.65	9.98E-04	3.99E-04	*2.33E-10	*1.61E-10								
SUM=	1.91E-02	3.20E-03	6.78E-03	5.24L-04	3.31L-02	7.65E-03	1.07L-02	1.10L-03	7.03L-02	1.42L-02	2.31L-02	2.45L-03

	1 PPM THORIUM				1 PPM URANIUM				1% POTASSIUM			
E (MEV)	PHI0*	PHI1*	PHI0*	PHI1*	PHI0*	PHI1*	PHI0*	PHI1*	PHI0*	PHI1*	PHI0*	PHI1*
0.10-0.15	2.03E-03	2.55E-04	1.77E-03	1.11E-04	6.38E-03	5.66E-04	3.99E-03	2.69E-04	1.07E-02	8.94E-04	7.46E-03	4.34E-04
0.15-0.20	1.52E-03	1.01E-04	8.94E-04	4.66E-05	3.44E-03	2.27E-04	2.03E-03	1.12E-04	5.74E-03	3.58E-04	4.27E-03	1.14E-04
0.20-0.25	1.09E-03	2.06E-04	5.12E-04	1.61E-05	2.48E-03	3.73E-04	1.16E-03	4.06E-05	3.91E-03	3.12E-04	2.73E-03	3.76E-05
0.25-0.30	7.17E-04	1.10E-04	2.77E-04	4.69E-05	1.69E-03	1.98E-04	5.96E-04	1.08E-04	3.07E-03	2.91E-04	1.67E-03	2.05E-04
0.30-0.35	5.99E-04	1.28E-04	1.59E-04	4.07E-05	1.37E-03	3.00E-04	3.36E-04	9.05E-05	2.53E-03	3.04E-04	9.47E-04	2.27E-04
0.35-0.40	4.85E-04	9.26E-05	9.95E-05	3.27E-05	1.19E-03	3.18E-04	2.08E-04	7.20E-05	2.17E-03	3.14E-04	6.66E-04	2.01E-04
0.40-0.45	4.01E-04	6.69E-05	6.52E-05	2.32E-05	9.63E-04	1.97E-04	1.34E-04	5.55E-05	1.66-E-03	2.19E-04	4.38E-04	1.67E-04
0.45-0.50	3.61E-04	1.00E-04	4.46E-05	1.93E-05	7.56E-04	2.01E-04	9.20E-05	4.22E-05	1.67E-03	3.21E-04	3.15E-04	1.37E-04
0.50-0.55	3.31E-04	1.03E-04	3.14E-05	1.44E-05	6.72E-04	1.97E-04	6.41E-05	3.19E-05	1.54E-03	3.42E-04	2.43E-04	1.11E-04
0.55-0.60	3.09E-04	1.37E-04	2.28E-05	1.15E-05	6.18E-04	1.99E-04	4.58E-05	2.41E-05	1.37E-03	3.17E-04	1.87E-04	8.93E-05
0.60-0.65	2.87E-04	6.07E-05	1.70E-05	9.06E-06	9.48E-04	3.49E-04	2.63E-05	1.40E-05	1.20E-03	3.16E-04	1.27E-04	7.19E-05
0.65-0.70	1.94E-04	8.08E-05	1.28E-05	7.06E-06	3.79E-04	1.13E-04	2.63E-05	1.51E-05	1.17E-03	3.11E-04	9.77E-05	5.72E-05
0.70-0.75	2.19E-04	7.90E-05	9.86E-06	5.54E-06	3.43E-04	1.07E-04	2.03E-05	1.20E-05	1.19E-03	3.07E-04	7.49E-05	4.69E-05
0.75-0.80	2.13E-04	8.11E-05	7.66E-06	4.44E-06	3.07E-04	1.03E-04	1.54E-05	9.61E-06	1.04E-03	3.03E-04	5.78E-05	3.67E-05
0.80-0.85	1.66E-04	6.82E-05	6.03E-06	3.50E-06	3.09E-04	1.03E-04	1.19E-05	7.70E-06	9.66E-04	3.03E-04	4.33E-05	2.91E-05
0.85-0.90	1.50E-04	6.03E-05	4.84E-06	2.94E-06	2.58E-04	8.68E-05	9.13E-06	6.08E-06	9.49E-04	2.98E-04	3.27E-05	2.28E-05
0.90-0.95	2.99E-04	1.32E-04	4.05E-06	2.49E-06	3.80E-04	1.11E-04	6.98E-06	4.78E-06	9.04E-04	2.94E-04	2.45E-05	1.72E-05
0.95-1.00	2.30E-04	1.04E-04	3.46E-06	2.19E-06	2.30E-04	8.03E-05	5.23E-06	3.67E-06	8.69E-04	2.93E-04	1.72E-05	1.26E-05
1.00-1.05	5.78E-03	1.72E-03	2.95E-04	1.91E-04	2.27E-04	8.18E-05	3.89E-06	2.70E-06	8.63E-04	2.92E-04	1.13E-05	8.97E-06
1.05-1.10	4.10E-03	1.09E-03	2.31E-04	1.65E-04	2.23E-04	8.24E-05	2.91E-06	2.11E-06	8.22E-04	2.92E-04	7.36E-06	6.07E-06
1.10-1.15	5.20E-03	1.02E-03	2.13E-04	1.63E-04	9.46E-04	2.48E-04	2.48E-06	1.75E-06	8.02E-04	2.91E-04	6.66E-06	4.92E-06
1.15-1.20	5.02E-03	1.96E-03	1.82E-04	1.23E-04	1.93E-04	7.43E-05	1.79E-06	1.34E-06	7.86E-04	2.91E-04	2.82E-06	2.31E-06
1.20-1.25	5.37E-03	1.70E-03	1.55E-04	1.06E-04	3.12E-04	1.30E-04	1.36E-06	1.04E-06	7.77E-04	2.90E-04	1.66E-06	1.24E-06
1.25-1.30	6.02E-03	1.46E-03	1.31E-04	9.09E-07	1.65E-04	6.33E-05	1.03E-06	7.68E-07	7.56E-04	2.90E-04	7.06E-07	5.72E-07
1.30-1.35	6.40E-03	1.40E-03	1.11E-04	7.74E-07	1.10E-04	4.24E-05	7.50E-07	5.74E-07	7.44E-04	2.91E-04	2.61E-07	2.05E-07
1.35-1.40	6.30E-03	1.39E-03	9.36E-07	6.56E-07	2.92E-04	1.44E-04	5.65E-07	4.50E-07	7.33E-04	2.93E-04	-7.32E-07	-6.78E-07
1.40-1.45	6.22E-03	1.38E-03	7.89E-07	5.58E-07	2.12E-04	8.73E-05	4.52E-07	3.67E-07	7.21E-04	2.95E-04	-7.17E-07	-6.74E-07
1.45-1.50	7.07E-03	3.00E-03	6.71E-07	4.78E-07	8.47E-05	3.42E-05	3.23E-07	2.63E-07	7.19E-04	6.27E-03	-2.14E-06	-1.66E-06
1.50-1.55	4.81E-03	1.63E-03	5.80E-07	4.18E-07	1.86E-04	7.59E-05	2.33E-07	1.73E-07				
1.55-1.60	1.11E-04	4.67E-05	9.22E-07	3.79E-07	1.49E-04	5.00E-05	1.61E-07	1.17E-07				
1.60-1.65	9.06E-05	3.96E-05	4.57E-07	3.14E-07	7.13E-05	2.58E-05	1.09E-07	7.69E-08				
1.65-1.70	3.19E-05	1.06E-05	3.09E-07	2.06E-07	1.21E-04	4.78E-05	7.42E-08	5.15E-08				
1.70-1.75	2.50E-05	8.07E-06	3.20E-07	2.03E-07	1.70E-04	7.01E-05	8.23E-08	6.46E-08				
1.75-1.80	2.56E-05	7.96E-06	2.77E-07	2.06E-07	6.05E-04	2.91E-04	6.89E-08	6.38E-08				
1.80-1.85	2.00E-05	9.17E-06	2.32E-07	1.73E-07	1.30E-04	5.49E-05	5.12E-08	4.72E-08				
1.85-1.90	2.03E-05	8.09E-06	1.93E-07	1.43E-07	6.66E-05	1.73E-05	4.08E-08	2.98E-08				
1.90-1.95	2.44E-05	7.77E-06	1.80E-07	1.18E-07	1.64E-05	5.38E-06	3.02E-08	2.20E-08				
1.95-2.00	2.42E-05	7.73E-06	1.31E-07	9.42E-08	1.63E-05	5.36E-06	2.05E-08	1.48E-08				
2.00-2.05	2.40E-05	7.70E-06	1.00E-07	7.76E-08	1.62E-05	5.36E-06	8.08E-09	6.22E-09				
2.05-2.10	2.38E-05	7.67E-06	8.46E-08	6.15E-08	1.62E-05	5.37E-06	-6.31E-09	-3.29E-09				
2.10-2.15	2.36E-05	7.63E-06	6.60E-08	4.82E-08	7.90E-05	3.16E-05	-1.73E-08	-1.06E-08				
2.15-2.20	2.35E-05	7.63E-06	5.30E-08	3.79E-08	1.36E-05	6.05E-06	-1.40E-08	-9.23E-09				
2.20-2.25	2.34E-05	7.60E-06	6.09E-08	2.89E-08	2.75E-04	1.12E-04	-9.90E-09	-6.17E-09				
2.25-2.30	2.32E-05	7.58E-06	2.32E-08	1.64E-08	2.68E-05	1.01E-05	-5.96E-09	-3.45E-09				
2.30-2.35	2.32E-05	7.58E-06	-1.60E-09	-7.26E-10	2.90E-06	1.00E-06	-3.80E-09	-2.54E-09				
2.35-2.40	2.31E-05	7.56E-06	-2.37E-08	-1.57E-08	2.97E-06	1.00E-06	-2.12E-09	-1.47E-09				
2.40-2.45	2.30E-05	7.53E-06	-3.76E-08	-2.53E-08	9.03E-05	3.03E-05	-6.03E-10	-6.31E-10				
2.45-2.50	2.30E-05	7.53E-06	-2.01E-08	-1.09E-08								
2.50-2.55	2.29E-05	7.51E-06	-1.71E-08	-1.15E-08								
2.55-2.60	2.28E-05	7.49E-06	-7.19E-09	-4.83E-09								
2.60-2.65	8.11E-04	3.19E-04	-3.95E-10	-2.66E-10								
SUM*	1.24E-02	2.79E-03	3.94E-03	4.32E-04	2.72E-02	8.10E-03	8.78E-03	9.69E-04	5.96E-02	1.27E-02	1.47E-02	2.08E-03

	1 PPM THORIUM				1 PPM URANIUM				1% POTASSIUM			
E (MEV)	PHI0+	PHI1+	PHI0-	PHI1-	PHI0+	PHI1+	PHI0-	PHI1-	PHI0+	PHI1+	PHI0-	PHI1-
0.10-0.15	2.36E-03	2.20E-04	1.46E-03	9.25E-05	5.30E-03	4.93E-04	3.28E-03	2.07E-04	9.69E-03	6.47E-04	6.41E-03	3.80E-04
0.15-0.20	1.25E-03	1.40E-04	7.46E-04	3.49E-05	2.82E-03	3.20E-04	1.68E-03	8.99E-05	4.93E-03	3.21E-04	3.68E-03	1.11E-04
0.20-0.25	8.02E-04	1.97E-04	4.32E-04	2.82E-05	1.94E-03	3.03E-04	9.50E-04	7.24E-05	3.34E-03	2.74E-04	2.50E-03	3.32E-05
0.25-0.30	5.95E-04	9.55E-05	2.34E-04	3.76E-05	1.93E-03	3.16E-04	5.00E-04	8.96E-05	2.65E-03	2.52E-04	1.44E-03	1.81E-05
0.30-0.35	4.94E-04	1.02E-04	1.34E-04	3.45E-05	1.13E-03	2.46E-04	2.82E-04	7.74E-05	2.20E-03	2.65E-04	8.43E-04	1.96E-05
0.35-0.40	3.84E-04	7.97E-05	8.37E-05	2.78E-05	9.58E-04	2.53E-04	1.73E-04	6.10E-05	1.87E-03	2.78E-04	5.41E-04	1.74E-05
0.40-0.45	3.38E-04	8.32E-05	5.49E-05	2.16E-05	7.11E-04	1.71E-04	1.13E-04	4.71E-05	1.63E-03	2.86E-04	3.66E-04	1.44E-05
0.45-0.50	3.03E-04	8.57E-05	3.74E-05	1.65E-05	6.35E-04	1.74E-04	7.61E-05	3.57E-05	1.45E-03	2.90E-04	2.56E-04	1.17E-05
0.50-0.55	2.79E-04	8.68E-05	2.63E-05	1.27E-05	5.67E-04	1.71E-04	5.28E-05	2.69E-05	1.31E-03	2.91E-04	1.85E-04	9.16E-06
0.55-0.60	2.96E-04	1.11E-04	1.90E-05	9.78E-06	5.19E-04	1.72E-04	3.76E-05	2.02E-05	1.19E-03	2.90E-04	1.36E-04	7.44E-06
0.60-0.65	1.78E-04	5.42E-05	1.40E-05	7.64E-06	7.30E-04	3.16E-04	2.80E-05	1.57E-05	1.19E-03	2.88E-04	1.03E-04	5.84E-06
0.65-0.70	1.66E-04	5.42E-05	1.06E-05	5.91E-06	3.20E-04	1.01E-04	2.12E-05	1.23E-05	1.02E-03	2.86E-04	7.81E-05	4.59E-06
0.70-0.75	1.82E-04	6.85E-05	8.07E-06	4.58E-06	2.93E-04	9.63E-05	1.59E-05	9.62E-06	9.54E-04	2.83E-04	5.86E-05	3.62E-06
0.75-0.80	1.75E-04	6.92E-05	6.22E-06	3.64E-06	3.20E-04	1.23E-04	1.20E-05	7.57E-06	9.00E-04	2.80E-04	4.38E-05	2.82E-06
0.80-0.85	1.38E-04	5.27E-05	4.83E-06	2.92E-06	2.50E-04	9.22E-05	9.08E-06	5.93E-06	8.50E-04	2.79E-04	3.23E-05	2.17E-06
0.85-0.90	1.32E-04	5.23E-05	3.84E-06	2.36E-06	2.18E-04	7.59E-05	6.70E-06	4.55E-06	8.15E-04	2.76E-04	2.31E-05	1.62E-06
0.90-0.95	2.33E-04	1.08E-04	3.24E-06	2.04E-06	2.52E-04	9.78E-05	4.92E-06	3.47E-06	7.83E-04	2.75E-04	1.56E-05	1.17E-06
0.95-1.00	1.07E-04	8.54E-05	2.77E-06	1.78E-06	1.98E-04	7.36E-05	3.48E-06	2.56E-06	7.52E-04	2.72E-04	1.02E-05	8.06E-07
1.00-1.05	5.09E-05	1.62E-05	2.33E-06	1.53E-06	1.95E-04	7.47E-05	2.43E-06	1.86E-06	7.31E-04	2.72E-04	6.22E-06	5.38E-07
1.05-1.10	5.30E-05	1.80E-05	1.95E-06	1.31E-06	1.90E-04	7.52E-05	1.73E-06	1.37E-06	7.09E-04	2.71E-04	3.47E-06	3.42E-07
1.10-1.15	4.63E-05	1.53E-05	1.62E-06	1.11E-06	4.30E-04	1.99E-04	1.40E-06	1.13E-06	8.91E-04	2.71E-04	1.83E-06	2.03E-07
1.15-1.20	4.43E-05	1.48E-05	1.35E-06	9.45E-07	1.63E-04	6.60E-05	9.98E-07	8.29E-07	6.70E-04	2.71E-04	9.66E-07	1.07E-07
1.20-1.25	4.67E-05	1.64E-05	1.12E-06	7.97E-07	2.52E-04	1.12E-04	7.22E-07	6.10E-07	6.61E-04	2.71E-04	4.83E-07	4.90E-07
1.25-1.30	4.08E-05	1.39E-05	9.23E-07	6.67E-07	1.39E-04	5.71E-05	5.20E-07	4.51E-07	6.47E-04	2.72E-04	2.11E-07	1.94E-07
1.30-1.35	3.90E-05	1.34E-05	7.55E-07	5.54E-07	1.02E-04	3.99E-05	3.59E-07	3.10E-07	6.35E-04	2.73E-04	5.00E-08	5.21E-08
1.35-1.40	3.81E-05	1.33E-05	6.17E-07	4.58E-07	2.36E-04	1.00E-04	2.73E-07	2.35E-07	6.24E-04	2.75E-04	-5.36E-07	-3.50E-07
1.40-1.45	3.73E-05	1.33E-05	5.06E-07	3.81E-07	1.73E-04	7.62E-05	2.05E-07	1.76E-07	6.12E-04	2.78E-04	-8.96E-07	-5.24E-07
1.45-1.50	6.63E-05	2.74E-05	4.20E-07	3.19E-07	7.39E-05	2.88E-05	1.39E-07	1.15E-07	7.43E-03	3.57E-03	-1.51E-06	-9.91E-07
1.50-1.55	3.69E-05	1.36E-05	3.57E-07	2.74E-07	1.53E-04	6.70E-05	9.57E-08	7.64E-08				
1.55-1.60	9.03E-05	3.91E-05	3.23E-07	2.51E-07	1.00E-04	4.59E-05	6.29E-08	4.84E-08				
1.60-1.65	8.02E-05	3.46E-05	2.79E-07	2.18E-07	6.21E-05	2.48E-05	3.97E-08	2.92E-08				
1.65-1.70	2.79E-05	1.01E-05	2.29E-07	1.82E-07	1.01E-04	4.34E-05	2.59E-08	1.85E-08				
1.70-1.75	2.31E-05	7.95E-06	1.88E-07	1.50E-07	1.46E-04	6.47E-05	2.33E-08	1.70E-08				
1.75-1.80	2.27E-05	7.85E-06	1.53E-07	1.23E-07	5.45E-04	2.50E-04	2.65E-08	1.65E-08				
1.80-1.85	2.47E-05	8.89E-06	1.24E-07	9.96E-08	1.12E-04	4.96E-05	2.08E-08	1.58E-08				
1.85-1.90	2.33E-05	8.30E-06	1.00E-07	7.96E-08	3.76E-05	1.57E-05	1.63E-08	1.25E-08				
1.90-1.95	2.18E-05	7.70E-06	8.02E-08	6.33E-08	1.45E-05	5.48E-06	1.16E-08	8.86E-09				
1.95-2.00	2.15E-05	7.65E-06	6.30E-08	4.92E-08	1.44E-05	5.47E-06	7.34E-09	5.51E-09				
2.00-2.05	2.14E-05	7.64E-06	4.93E-08	3.81E-08	1.43E-05	5.48E-06	-2.01E-10	3.71E-10				
2.05-2.10	2.12E-05	7.61E-06	3.78E-08	2.68E-08	1.42E-05	5.50E-06	-1.01E-08	-6.03E-09				
2.10-2.15	2.10E-05	7.59E-06	2.68E-08	2.16E-08	6.47E-05	2.80E-05	-1.74E-08	-1.08E-08				
2.15-2.20	2.09E-05	7.59E-06	2.29E-08	1.68E-08	1.19E-05	4.63E-06	-1.44E-08	-9.03E-09				
2.20-2.25	2.07E-05	7.57E-06	1.79E-08	1.27E-08	2.23E-04	9.79E-05	-9.62E-09	-6.14E-09				
2.25-2.30	2.06E-05	7.57E-06	6.77E-09	4.87E-09	2.10E-05	9.19E-06	-5.64E-09	-3.71E-09				
2.30-2.35	2.05E-05	7.58E-06	-1.17E-08	-7.57E-09	2.62E-06	1.01E-06	-3.58E-09	-2.38E-09				
2.35-2.40	2.04E-05	7.58E-06	-2.79E-08	-1.84E-08	2.61E-06	1.01E-06	-2.00E-09	-1.33E-09				
2.40-2.45	2.03E-05	7.57E-06	-3.76E-08	-2.50E-08	7.67E-05	3.38E-05	-6.06E-10	-4.02E-10				
2.45-2.50	2.03E-05	7.59E-06	-2.76E-08	-1.85E-08								
2.50-2.55	2.02E-05	7.61E-06	-1.69E-08	-1.12E-08								
2.55-2.60	2.01E-05	7.60E-06	-7.11E-09	-4.73E-09								
2.60-2.65	6.65E-04	2.82E-04	-3.91E-10	-2.60E-10								
SUM=	1.03E-02	2.40E-03	3.29E-03	3.50E-04	2.24E-02	5.20E-03	7.25E-03	7.96E-04	5.08E-02	1.15E-02	1.67E-02	1.74E-03

	1 PPM THORIUM				1 PPM URANIUM				1% POTASSIUM			
E (MEV)	PM10+	PM11+	PM10-	PM11-	PM10+	PM11+	PM10-	PM11-	PM10+	PM11+	PM10-	PM11-
0.10-0.15	1.96E-03	1.88E-04	1.20E-03	7.72E-05	6.40E-03	6.23E-04	2.69E-03	1.72E-04	8.24E-03	5.91E-04	5.49E-03	3.29E-04
0.15-0.20	1.03E-03	1.21E-04	6.24E-04	2.96E-05	2.31E-03	2.67E-04	1.39E-03	7.26E-05	4.23E-03	2.88E-04	3.15E-03	9.12E-05
0.20-0.25	7.17E-04	1.21E-04	3.64E-04	2.34E-05	1.59E-03	2.45E-04	7.94E-04	5.88E-05	2.88E-03	2.37E-04	2.14E-03	2.97E-05
0.25-0.30	4.95E-04	7.03E-05	1.94E-04	3.17E-05	1.25E-03	2.50E-04	4.19E-04	7.59E-05	2.27E-03	2.17E-04	1.21E-03	1.59E-04
0.30-0.35	4.10E-04	8.27E-05	1.14E-04	2.94E-05	9.81E-04	2.00E-04	2.37E-04	6.63E-05	1.87E-03	2.31E-04	7.13E-04	1.73E-04
0.35-0.40	3.24E-04	6.88E-05	7.86E-05	2.38E-05	7.82E-04	2.02E-04	1.49E-04	5.28E-05	1.62E-03	2.45E-04	4.56E-04	1.51E-04
0.40-0.45	2.63E-04	7.07E-05	4.43E-05	1.85E-05	6.00E-04	1.46E-04	9.38E-05	4.01E-05	1.41E-03	2.55E-04	3.06E-04	1.24E-04
0.45-0.50	2.54E-04	7.23E-05	3.15E-05	1.42E-05	5.35E-04	1.49E-04	6.30E-05	3.03E-05	1.28E-03	2.60E-04	2.11E-04	9.96E-05
0.50-0.55	2.30E-04	7.27E-05	2.21E-05	1.08E-05	4.79E-04	1.46E-04	4.35E-05	2.26E-05	1.13E-03	2.62E-04	1.52E-04	7.91E-05
0.55-0.60	2.40E-04	9.04E-05	1.59E-05	8.33E-06	4.30E-04	1.46E-04	3.07E-05	1.68E-05	1.03E-03	2.62E-04	1.11E-04	6.19E-05
0.60-0.65	1.52E-04	6.76E-05	1.17E-05	6.44E-06	3.71E-04	2.50E-04	2.29E-05	1.30E-05	9.53E-04	2.61E-04	8.35E-05	4.78E-05
0.65-0.70	1.42E-04	6.75E-05	8.71E-06	4.92E-06	2.74E-04	8.87E-05	1.72E-05	9.69E-06	8.87E-04	2.60E-04	6.26E-05	3.64E-05
0.70-0.75	1.52E-04	5.82E-05	6.50E-06	3.77E-06	2.52E-04	8.51E-05	1.27E-05	7.70E-06	8.29E-04	2.57E-04	4.64E-05	2.68E-05
0.75-0.80	1.45E-04	5.04E-05	5.02E-06	2.96E-06	2.74E-04	1.06E-04	9.41E-06	5.94E-06	7.81E-04	2.55E-04	3.36E-05	2.16E-05
0.80-0.85	1.16E-04	4.55E-05	3.83E-06	2.36E-06	2.20E-04	8.12E-05	6.91E-06	4.55E-06	7.43E-04	2.54E-04	2.47E-05	1.60E-05
0.85-0.90	1.11E-04	4.49E-05	3.01E-06	1.90E-06	1.89E-04	6.85E-05	4.89E-06	3.38E-06	7.07E-04	2.51E-04	1.80E-05	1.16E-05
0.90-0.95	1.04E-04	8.82E-05	2.50E-06	1.67E-06	2.12E-04	8.55E-05	3.62E-06	2.49E-06	6.74E-04	2.50E-04	1.32E-05	7.78E-06
0.95-1.00	1.48E-04	7.08E-05	2.22E-06	1.45E-06	1.71E-04	6.62E-05	2.27E-06	1.77E-06	6.51E-04	2.48E-04	9.97E-06	5.06E-06
1.00-1.05	4.58E-05	1.49E-05	1.05E-04	1.24E-06	1.07E-04	6.71E-05	1.46E-06	1.24E-06	6.32E-04	2.48E-04	3.19E-06	3.18E-06
1.05-1.10	4.63E-05	1.63E-05	1.52E-06	1.04E-06	1.63E-04	6.74E-05	9.72E-07	8.77E-07	6.14E-04	2.47E-04	1.47E-06	1.92E-06
1.10-1.15	4.09E-05	1.42E-05	1.24E-06	6.65E-07	3.03E-04	1.66E-04	7.85E-07	7.20E-07	5.95E-04	2.47E-04	6.15E-07	1.07E-06
1.15-1.20	3.92E-05	1.37E-05	1.00E-06	7.21E-07	1.38E-04	5.66E-05	5.21E-07	5.10E-07	5.81E-04	2.47E-04	2.77E-07	6.95E-07
1.20-1.25	4.09E-05	1.51E-05	8.07E-07	5.95E-07	2.06E-04	9.59E-05	3.55E-07	3.67E-07	5.67E-04	2.48E-04	1.65E-07	1.94E-07
1.25-1.30	3.62E-05	1.31E-05	8.40E-07	4.06E-07	1.10E-04	5.09E-05	2.43E-07	2.57E-07	5.54E-04	2.48E-04	5.85E-08	6.66E-08
1.30-1.35	3.46E-05	1.26E-05	5.03E-07	3.93E-07	8.69E-05	3.46E-05	1.60E-07	1.65E-07	5.42E-04	2.50E-04	8.96E-09	1.11E-08
1.35-1.40	3.30E-05	1.25E-05	3.95E-07	3.17E-07	1.93E-04	9.12E-05	1.18E-07	1.22E-07	5.31E-04	2.52E-04	-1.67E-07	-2.25E-07
1.40-1.45	3.31E-05	1.25E-05	3.13E-07	2.57E-07	1.42E-04	6.59E-05	8.72E-08	8.82E-08	5.20E-04	2.55E-04	-3.14E-07	-2.05E-07
1.45-1.50	5.56E-05	2.62E-05	2.52E-07	2.12E-07	6.45E-05	2.69E-05	5.63E-08	5.28E-08	5.84E-04	2.96E-03	-4.64E-04	-6.25E-04
1.50-1.55	3.84E-05	1.87E-05	2.11E-07	1.79E-07	1.26E-04	5.86E-05	3.73E-08	3.29E-08				
1.55-1.60	7.44E-05	3.40E-05	1.93E-07	1.64E-07	9.05E-05	4.10E-05	2.34E-08	1.94E-08				
1.60-1.65	6.68E-05	3.00E-05	1.63E-07	1.41E-07	5.42E-05	2.33E-05	1.39E-08	1.07E-08				
1.65-1.70	2.45E-05	9.43E-06	1.29E-07	1.15E-07	8.45E-05	3.88E-05	8.68E-09	6.41E-09				
1.70-1.75	2.07E-05	7.64E-06	1.02E-07	9..8E-08	1.20E-04	5.67E-05	8.31E-09	6.34E-09				
1.75-1.80	2.03E-05	7.55E-06	8.04E-08	7.26E-08	4.38E-04	2.13E-04	9.49E-09	7.57E-09				
1.80-1.85	2.19E-05	8.43E-06	6.34E-08	5.46E-08	9.10E-05	4.30E-05	8.05E-09	6.51E-09				
1.85-1.90	2.07E-05	7.94E-06	4.93E-08	4.33E-08	3.15E-05	1.41E-05	6.21E-09	5.07E-09				
1.90-1.95	1.94E-05	7.42E-06	3.84E-08	3.32E-08	1.28E-05	5.24E-06	4.28E-09	3.48E-09				
1.95-2.00	1.92E-05	7.39E-06	2.98E-08	2.49E-08	1.27E-05	5.24E-06	2.52E-09	2.08E-09				
2.00-2.05	1.91E-05	7.38E-06	2.20E-08	1.83E-08	1.26E-05	5.24E-06	-2.23E-09	-1.19E-09				
2.05-2.10	1.89E-05	7.36E-06	1.62E-08	1.32E-08	1.25E-05	5.29E-06	-9.10E-09	-5.61E-09				
2.10-2.15	1.87E-05	7.35E-06	1.19E-08	9.30E-09	5.33E-05	2.47E-05	-1.43E-08	-8.69E-09				
2.15-2.20	1.86E-05	7.36E-06	9.58E-09	7.27E-09	1.05E-05	6.47E-06	-1.16E-08	-7.31E-09				
2.20-2.25	1.86E-05	7.35E-06	7.57E-09	5.44E-09	1.82E-04	6.51E-05	-7.79E-09	-4.96E-09				
2.25-2.30	1.83E-05	7.35E-06	6.81E-10	6.00E-10	1.83E-05	8.29E-06	-6.56E-09	-2.99E-09				
2.30-2.35	1.82E-05	7.17E-06	-1.30E-08	-8.53E-09	2.31E-06	9.77E-07	-2.89E-09	-1.91E-09				
2.35-2.40	1.81E-05	7.10E-06	-2.47E-08	-1.63E-08	2.30E-06	9.82E-07	-1.62E-09	-1.07E-09				
2.40-2.45	1.80E-05	7.10E-06	-3.15E-08	-2.09E-08	6.47E-05	2.96E-05	-4.90E-10	-3.24E-10				
2.45-2.50	1.79E-05	7.42E-06	-2.32E-08	-1.54E-08								
2.50-2.55	1.78E-05	7.45E-06	-1.41E-08	-9.33E-09								
2.55-2.60	1.77E-05	7.47E-06	-5.94E-09	-3.93E-09								
2.60-2.65	5.49E-04	2.48E-04	-3.27E-10	-2.16E-10								
SUM:	8.59E-03	2.04E-03	2.74E-03	2.99E-04	1.85E-02	4.40E-03	6.00E-03	6.61E-04	4.31E-02	1.01E-02	1.42E-02	1.48E-03

E (MEV)	1 PPM THORIUM				1 PPM URANIUM				1% POTASSIUM			
	PM10+	PM11+	PM10-	PM11-	PM10+	PM11+	PM10-	PM11-	PM10+	PM11+	PM10-	PM11-
0.10-0.15	1.63E-03	1.59E-04	9.94E-04	6.45E-05	3.65E-03	3.59E-04	2.21E-03	1.43E-04	7.10E-04	5.32E-04	6.70E-04	2.82E-04
0.15-0.20	8.50E-04	9.02E-05	5.21E-04	2.41E-05	1.90E-03	2.17E-04	1.15E-03	5.92E-05	3.42E-04	2.46E-04	2.70E-04	7.53E-05
0.20-0.25	5.07E-04	9.35E-05	3.07E-04	1.93E-05	1.31E-03	1.98E-04	6.62E-04	4.79E-05	2.45E-04	2.04E-04	1.84E-04	2.64E-05
0.25-0.30	4.13E-04	6.41E-05	1.67E-04	2.69E-05	1.02E-03	1.48E-04	3.50E-04	6.43E-05	1.95E-04	1.66E-04	1.04E-04	1.40E-05
0.30-0.35	3.42E-04	6.73E-05	9.01E-05	2.52E-05	7.02E-04	1.03E-04	1.98E-04	5.65E-05	1.63E-04	2.01E-04	6.03E-05	1.51E-04
0.35-0.40	2.74E-04	5.76E-05	5.96E-05	2.04E-05	6.43E-04	1.03E-04	1.21E-04	4.44E-05	1.40E-04	2.15E-04	3.83E-05	1.31E-04
0.40-0.45	2.40E-04	5.97E-05	3.89E-05	1.59E-05	5.04E-04	1.25E-04	7.78E-05	3.41E-05	1.22E-04	2.25E-04	2.50E-05	1.07E-04
0.45-0.50	2.14E-04	6.07E-05	2.64E-05	1.21E-05	4.51E-04	1.26E-04	5.20E-05	2.56E-05	1.09E-04	2.31E-04	1.77E-05	8.50E-05
0.50-0.55	1.93E-04	6.07E-05	1.84E-05	9.23E-06	4.04E-04	1.26E-04	3.55E-05	1.88E-05	9.82E-05	2.34E-04	1.26E-05	6.67E-05
0.55-0.60	1.98E-04	7.35E-05	1.32E-05	7.06E-06	3.69E-04	1.42E-04	2.49E-05	1.38E-05	8.98E-05	2.34E-04	9.13E-06	5.15E-05
0.60-0.65	1.31E-04	4.14E-05	9.67E-06	5.40E-06	4.52E-04	1.98E-04	1.86E-05	1.07E-05	8.27E-05	2.34E-04	6.79E-06	3.90E-05
0.65-0.70	1.22E-04	4.12E-05	7.13E-06	4.06E-06	2.35E-04	7.75E-05	1.40E-05	8.10E-06	7.70E-05	2.33E-04	5.01E-06	2.99E-05
0.70-0.75	1.20E-04	4.92E-05	5.32E-06	3.06E-06	2.16E-04	7.46E-05	1.01E-05	6.11E-06	7.17E-05	2.31E-04	3.61E-06	2.22E-05
0.75-0.80	1.21E-04	4.92E-05	4.00E-06	2.30E-06	2.30E-04	9.00E-05	7.33E-06	4.63E-06	6.78E-05	2.29E-04	2.54E-06	1.64E-05
0.80-0.85	9.07E-05	3.91E-05	3.00E-06	1.88E-06	1.88E-04	7.10E-05	5.23E-06	3.45E-06	6.48E-05	2.28E-04	1.72E-06	1.17E-05
0.85-0.90	9.32E-05	3.84E-05	2.33E-06	1.51E-06	1.64E-04	6.10E-05	3.56E-06	2.48E-06	6.12E-05	2.26E-04	1.09E-06	7.92E-06
0.90-0.95	1.47E-04	7.10E-05	2.04E-06	1.34E-06	1.00E-04	7.42E-05	2.35E-06	1.76E-06	5.87E-05	2.25E-04	6.42E-06	5.12E-06
0.95-1.00	1.18E-04	5.73E-05	1.79E-06	1.18E-06	1.47E-04	5.89E-05	1.44E-06	1.21E-06	5.63E-04	2.23E-04	3.77E-06	3.14E-06
1.00-1.05	3.98E-05	1.36E-05	1.67E-06	9.92E-07	1.44E-04	5.95E-05	8.37E-07	8.17E-07	5.63E-04	2.23E-04	1.94E-06	1.87E-06
1.05-1.10	4.05E-05	1.48E-05	1.10E-06	8.20E-07	1.40E-04	5.98E-05	5.10E-07	5.63E-07	5.28E-04	2.22E-04	4.97E-07	1.09E-06
1.10-1.15	3.62E-05	1.30E-05	9.30E-07	8.70E-07	2.75E-04	1.38E-04	4.10E-07	4.08E-07	5.14E-04	2.22E-04	1.01E-07	5.81E-07
1.15-1.20	3.40E-05	1.26E-05	7.30E-07	5.44E-07	1.17E-04	5.15E-05	2.44E-07	3.16E-07	4.99E-04	2.23E-04	5.61E-08	2.36E-07
1.20-1.25	3.59E-05	1.37E-05	5.73E-07	4.40E-07	1.70E-04	8.18E-05	1.55E-07	2.20E-07	4.83E-04	2.23E-04	3.59E-08	7.78E-08
1.25-1.30	3.21E-05	1.20E-05	4.36E-07	3.51E-07	1.00E-04	4.50E-05	1.00E-07	1.47E-07	4.73E-04	2.24E-04	1.47E-08	2.15E-08
1.30-1.35	3.00E-05	1.17E-05	3.27E-07	2.77E-07	7.73E-05	3.44E-05	6.35E-08	8.83E-08	4.63E-04	2.25E-04	*1.12E-07	1.21E-08
1.35-1.40	3.01E-05	1.16E-05	2.44E-07	2.18E-07	1.58E-04	7.01E-05	6.62E-08	6.26E-08	4.59E-04	2.26E-04	*2.19E-07	*1.36E-07
1.40-1.45	2.94E-05	1.16E-05	1.86E-07	1.73E-07	1.17E-04	5.68E-05	3.36E-08	4.41E-08	4.63E-04	2.29E-04	*1.89E-07	*1.23E-07
1.45-1.50	4.70E-05	2.12E-05	1.45E-07	1.30E-07	5.63E-05	2.47E-05	2.14E-08	2.40E-08	4.59E-04	2.45E-04	*5.78E-07	*3.78E-07
1.50-1.55	3.06E-05	1.17E-05	1.18E-07	1.17E-07	1.05E-04	5.09E-05	1.38E-08	1.40E-08				
1.55-1.60	4.17E-05	2.94E-05	1.09E-07	1.07E-07	7.63E-05	3.83E-05	8.32E-09	7.65E-09				
1.60-1.65	5.47E-05	2.59E-05	9.11E-08	9.10E-08	4.72E-05	2.15E-05	4.68E-09	3.64E-09				
1.65-1.70	2.16E-05	8.72E-06	8.07E-08	7.19E-08	7.12E-05	3.45E-05	2.81E-09	2.16E-09				
1.70-1.75	1.05E-05	7.22E-06	5.25E-08	5.59E-08	9.93E-05	4.96E-05	2.07E-09	2.33E-09				
1.75-1.80	1.01E-05	7.14E-06	3.97E-08	4.26E-08	3.53E-04	1.81E-04	1.51E-09	3.03E-09				
1.80-1.85	1.94E-05	7.09E-06	3.06E-08	3.20E-08	7.47E-05	3.70E-05	1.00E-09	2.63E-09				
1.85-1.90	1.84E-05	7.07E-06	2.31E-08	2.33E-08	2.06E-05	1.06E-05	2.28E-09	2.01E-09				
1.90-1.95	1.74E-05	7.03E-06	1.75E-08	1.72E-08	1.13E-05	6.93E-06	1.52E-09	1.36E-09				
1.95-2.00	1.72E-05	7.01E-06	1.20E-08	1.20E-08	1.12E-05	6.93E-06	8.19E-10	7.10E-10				
2.00-2.05	1.78E-05	7.01E-06	9.45E-09	8.01E-09	1.11E-05	6.95E-06	*2.24E-09	*1.41E-09				
2.05-2.10	1.68E-05	7.00E-06	6.69E-09	5.91E-09	1.10E-05	6.99E-06	*7.07E-09	*4.36E-09				
2.10-2.15	1.67E-05	6.99E-06	4.74E-09	3.97E-09	6.42E-05	2.16E-05	*1.06E-08	*6.40E-09				
2.15-2.20	1.66E-05	7.00E-06	3.05E-09	3.05E-09	9.22E-06	4.22E-06	*8.66E-09	*5.41E-09				
2.20-2.25	1.64E-05	7.00E-06	3.09E-09	2.26E-09	1.50E-04	7.37E-05	*5.79E-09	*3.68E-09				
2.25-2.30	1.63E-05	7.00E-06	*1.67E-09	*1.06E-09	1.54E-05	7.41E-06	*3.41E-09	*2.23E-09				
2.30-2.35	1.62E-05	7.00E-06	*1.12E-08	*7.36E-09	2.04E-06	9.49E-07	*2.17E-09	*1.43E-09				
2.35-2.40	1.61E-05	7.00E-06	*1.90E-08	*1.29E-08	2.03E-06	9.35E-07	*1.41E-09	*7.47E-10				
2.40-2.45	1.60E-05	7.05E-06	*2.43E-08	*1.60E-08	5.36E-05	2.58E-05	*3.67E-10	*2.41E-10				
2.45-2.50	1.59E-05	7.10E-06	*1.70E-08	*1.10E-08								
2.50-2.55	1.58E-05	7.14E-06	*1.08E-08	*7.15E-09								
2.55-2.60	1.57E-05	7.16E-06	*4.57E-09	*3.01E-09								
2.60-2.65	4.56E-04	2.17E-04	*2.51E-10	*1.66E-10								
SUM=	7.18E-03	1.74E-03	2.20E-03	2.91E-04	1.54E-02	7.71E-03	4.95E-03	5.49E-04	1.67E-02	8.81E-03	1.21E-04	1.70E-04

Table 7

Absorbed dose rates D(z) in air of the density 0.001293 g/cm^3 resulting from unit abundances of thorium, uranium, and potassium in the ground material (granite)

z(m)	D(z) (n rad/h)		
	1 ppm Th	1 ppm U	1 % K
0	0.277	0.570	1.37
1	0.271	0.556	1.34
25	0.204	0.415	1.02
50	0.161	0.324	0.806
75	0.130	0.258	0.653
100	0.106	0.209	0.538
125	0.0877	0.171	0.447
150	0.0731	0.141	0.374
175	0.0612	0.117	0.314
200	0.0516	0.0974	0.264

Table 8

Specific gamma-ray emissions Q_i for the natural radioelements and mass attenuation coefficients for use in the calculation of a flux of unscattered gamma rays

Gamma-ray source	E_i (MeV)	Q_i ($\gamma \cdot s^{-1} \cdot g^{-1}$)	Mass attenuation coefficient ($cm^2 \cdot g^{-1}$)		
			Granite	Soil	Air
1 ppm Th	0.2386	$1.85 \cdot 10^{-3}$	0.1153	0.1165	0.1149
	0.3385	$5.04 \cdot 10^{-4}$	0.1011	0.1023	0.1014
	0.5107	$3.69 \cdot 10^{-4}$	0.0857	0.0867	0.0862
	0.5831	$1.23 \cdot 10^{-3}$	0.0810	0.0820	0.0814
	0.7272	$2.87 \cdot 10^{-3}$	0.0733	0.0742	0.0738
	0.9111	$1.19 \cdot 10^{-3}$	0.0660	0.0668	0.0664
	0.9667	$9.43 \cdot 10^{-4}$	0.0642	0.0650	0.0646
	1.5881	$1.89 \cdot 10^{-4}$	0.0500	0.0506	0.0502
	2.6147	$1.47 \cdot 10^{-3}$	0.0388	0.0391	0.0385
1 ppm U	0.2952	$2.19 \cdot 10^{-3}$	0.1066	0.1078	0.1068
	0.3520	$4.28 \cdot 10^{-3}$	0.0996	0.1008	0.0999
	0.6094	$5.26 \cdot 10^{-3}$	0.0794	0.0804	0.0799
	1.1204	$1.77 \cdot 10^{-3}$	0.0596	0.0604	0.0600
	1.2382	$6.85 \cdot 10^{-4}$	0.0567	0.0574	0.0570
	1.3778	$5.62 \cdot 10^{-4}$	0.0537	0.0544	0.0540
	1.7647	$1.80 \cdot 10^{-3}$	0.0473	0.0479	0.0475
	2.2045	$5.75 \cdot 10^{-4}$	0.0423	0.0427	0.0422
	2.4480	$1.83 \cdot 10^{-4}$	0.0401	0.0405	0.0399
1% K	1.4608	$3.30 \cdot 10^{-2}$	0.0522	0.528	0.0524